Ethylene Receptor Gain- and Loss-of-function Mutants Reveal an ETR1-dependent Transcriptional Network in Roots

Running head: ETR1-dependent gene regulatory networks in roots

Alexandria F. Harkey[1*], Maleana G. Khoury[1*], Joëlle K. Mühlemann[1,2], Amy L. Olex[3], Maarten Houben[1,2], Brad M. Binder[4], Gloria K. Muday[1]

[1] Wake Forest University, Winston-Salem, NC

[2] KU Leuven, Belgium

[3] Virginia Commonwealth University, Richmond, VA

[4] University of Tennessee, Knoxville, TN

*Co-first authors

One sentence summary: Genome-wide transcriptional responses in *etr1* receptor gain- and loss-of-function mutants reveal an ethylene-mediated ETR1-dependent gene regulatory network that modulates root development.

Abstract

In Arabidopsis, a family of five receptors mediates ethylene responses in distinct tissues and cell types, with Ethylene Response 1 (ETR1) controlling ethylene-mediated increases in root hair proliferation and decreases in lateral root formation. To define the ETR1-dependent gene regulatory network (GRN) controlling root development, we profiled the transcriptome of roots from Col-0 seedlings and the *etr1-3* gain-of-function and *etr1-7* loss-of-function mutants in the presence and absence of ethylene or ACC treatment after 1, 4, and 24 hours. We identified 4,522 DE transcripts in Col-0 roots whose abundance changed in response to ethylene and/or ACC treatment with larger magnitude changes induced by ethylene. There were 961 genes regulated similarly by both treatments in at least one time point . We identified 553 transcripts that were ETR1-dependent, defined by the absence of response to ethylene and/or ACC treatment in the ethylene-insensitive *etr1-3* mutant and altered transcript abundance in the constitutive-signaling *etr1-7* mutant in the absence of ethylene and/or ACC relative to untreated Col-0. Six ETR1-dependent transcripts are predicted to encode transcription factors: *ANAC058*, *LRP1*, *MYB9*, *MYB52*, *MYB93*, and *RAP2.6L*. We examined ACC-modulated root development in plants with mutations in these genes, revealing roles of these proteins in regulating root development. Using published TF target data, we found TFs that are both EIN3-regulated and EIN3-independent with members of both groups regulating root development. Together, these findings reveal features of an ETR1-dependent GRN controlling root growth and development.

Introduction

Ethylene is a gaseous hormone that modulates growth and development throughout a plant's life cycle, from seed germination to senescence, and controls responses to both biotic and abiotic stress (Abeles et al. 1992; Van de Poel et al. 2015). In young, etiolated seedlings, ethylene induces a triple response: reduced hypocotyl and root elongation, thickening of the hypocotyl, and exaggeration of the apical hook. This triple response phenotype has been the basis of mutant screens in *Arabidopsis thaliana* that have identified key components of the ethylene signaling pathway with ethylene-insensitive or constitutive ethylene signaling phenotypes (Schaller and Kieber 2002). Ethylene also has profound effects on root development, including inhibition of primary root elongation and lateral root formation and stimulation of root hair initiation and elongation (Negi et al. 2008; Lewis et al. 2011; Feng et al. 2017; Harkey et al. 2018; Qin, He, and Huang 2019). Many of the proteins that were identified based on their functions in ethylene signaling in etiolated hypocotyls also modulate root development (Khoury et al. 2024), but with distinct developmental effects downstream of each receptor (Harkey et al. 2018).

Ethylene functions through direct binding to members of a family of transmembrane receptors that span the lipid bilayer of endoplasmic reticulum and the Golgi apparatus (Schaller and Kieber 2002; Binder 2020). These receptors are negative regulators of the pathway, such that binding of ethylene to these receptors removes repression of the pathway, which initiates a signaling cascade that activates or represses expression of genes, with distinct transcriptional responses depending on the tissue type and growth conditions (Chang et al. 2013; Harkey et al. 2018, 2019). In Arabidopsis, five receptor isoforms have been identified: Ethylene Response 1 (ETR1), ETR2, Ethylene Insensitive 4 (EIN4), Ethylene Response Sensor 1 (ERS1), and ERS2 (Chang et al. 1993; Schaller and Bleecker 1995; Hua and Meyerowitz 1998; Hua et al. 1998; Sakai

et al. 1998; Binder 2020). Unlike most canonical signaling pathways, however, ethylene receptors are active in the unbound state. In the absence of ethylene, these receptors activate the Raf-like serine/threonine protein kinase Constitutive Triple Response 1 (CTR1), destabilizing EIN3 and EIN3-like (EIL) transcription factors (TFs) and blocking changes in gene expression downstream of these TFs (An et al. 2010; Binder 2020; Dolgikh et al. 2019). In the bound state, however, the ethylene receptors lead to stabilization of EIN3 and EIL TFs in an EIN2-dependent manner (Alonso et al. 1999; An et al. 2010; Huang et al. 2003; Kieber et al. 1993; Qiao et al. 2009), leading to genome-wide changes in transcript abundance (Chang et al. 2013; Harkey et al. 2018). Downstream of EIN3/EIL are ethylene response factors (ERFs) and ethylene response DNA-binding factors (EDFs) that further mediate transcription, consistent with the existence of tissue-specific gene regulatory networks (GRNs) (Wang et al. 2002).

The function of ethylene signaling proteins in controlling root architecture has been examined (Khoury et al. 2024). EIN2 is required for root developmental responses to ethylene and its immediate precursor 1-aminocyclopropane-1-carboxylic acid, or ACC (Alonso and Stepanova 2004; Negi et al. 2008). The *ctr1-1* mutant was demonstrated to have constitutive-ethylene-signaling root phenotypes, with this mutant having shorter primary roots and increased root hair proliferation compared to Col-0 seedlings in the absence of ethylene (Hua and Meyerowitz 1998; Kieber et al. 1993; Masucci and Schiefelbein 1996; Rahman et al. 2000), suggesting its presence is required to suppress the pathway in the absence of ethylene. EIN3 and its homolog EIL1 function in ethylene-dependent root hair formation, with the *ein3eil1* double mutant having reduced ACC-induction of root hair proliferation (Feng et al. 2017). However, root developmental responses to ethylene can still be observed in the *ein3* and *ein3eil1* mutants (Chang et al. 2013; Harkey et al. 2018), suggesting that additional TFs may participate in these ethylene responses.

The five ethylene receptors in Arabidopsis each elicit distinct ethylene responses (Shakeel et al. 2013), partially due to differences in receptor subunit structure and receptor dimerization (Berleth et al. 2019). ETR1 was found to be the main receptor controlling inhibition of ethylene perception by silver nitrate, nutational bending of hypocotyls, and remodeling of root architecture (Harkey et al. 2018; McDaniel and Binder 2012). In Arabidopsis, ETR1 positively regulates nutational bending (Binder et al. 2006), while the other four receptors negatively regulate this process (Kim et al. 2011). In roots, using a series of single and multiple loss-of-function (LOF) and gain-of-function (GOF) mutants, only ETR1 was needed for the inhibition of lateral root formation by ACC (Harkey et al. 2018). The inhibition of lateral root formation by ACC was lost in the GOF, ethylene-insensitive mutant *etr1-3,* which had significantly more lateral roots than wild type in the presence and absence of ACC. The LOF, constitutive-signaling mutant *etr1-7* had significantly fewer lateral roots than wild type in the presence and absence of ACC. ETR1 also has a central role in the inhibition of primary root elongation and stimulation of root hair formation by ACC, consistent with ETR1 playing the most substantial role in modulating ethylene-mediated root remodeling (Harkey et al. 2018). Nevertheless, while it has been demonstrated that elevated levels of ethylene remodel the root transcriptome (Harkey et al. 2018, 2019; Stepanova et al. 2007), the GRN downstream of the ETR1 receptor has not yet been identified in roots.

To identify the ETR1-dependent GRN controlling root growth and development, we performed an RNA-Seq analysis in roots from light-grown seedlings using Col-0 and ETR1 receptor GOF (*etr1-3*) and LOF (*etr1-7*) mutants treated with and without ethylene and ACC for 1, 4, and 24 hours. We identified a core set of genes regulated by both ethylene and ACC. We also identified a subgroup of these transcripts that were dependent on ETR1, as they had altered expression in untreated *etr1-7* (as compared to Col-0) and their responses to ACC and/or ethylene

were lost in both *etr* mutants. Of the ETR1-dependent transcripts, many encoded proteins that putatively functioned as TFs, suggesting candidates for a GRN downstream of ETR1. We examined root phenotypes of mutants for six genes predicted to encode TFs and whose changes in transcript abundance were ETR1-dependent and responded to ACC treatment over time in a previously published time course transcriptional dataset (Harkey et al. 2018). We uncovered novel roles for some of these genes in the inhibition of lateral root formation or the stimulation of root hair initiation by ACC treatment and validated published phenotypes for others. Lastly, we overlapped these results with publicly available ChIP- and DAP-Seq data to place genes in an ETR1-dependent GRN downstream of ethylene signaling in roots.

Results

Previous experiments informed experimental design, including selection of doses of ethylene and ACC and treatment times for transcriptome analyses

A goal of this work was to examine the changes in the transcriptome profiles of ethylene- and ACC-treated roots of Col-0, *etr1-3,* and *etr1-7* seedlings to determine the extent of overlap between the receptor-mediated transcriptional responses to these molecules. Based on previous evidence that ACC and ethylene act through distinct signaling pathways in some tissues (Mou et al. 2020; Yin et al. 2019), we hypothesized that a similar scenario occurs in roots. As a first step, we determined the concentration of ethylene that yielded moderate root hair proliferation similar to that induced by 0.75 µM ACC, by examining root hairs in Col-0 seedlings treated with a range of ethylene levels for 24 hours (Figure 1A). The 0.3 ppm ethylene concentration appeared to induce root hair proliferation to a similar degree as 0.75 µM ACC. Therefore, we selected 0.3 ppm ethylene and 0.75 µM ACC for this RNA-Seq analysis.

We compared the effects of 24 hours of treatment with ethylene or ACC at these doses on the proliferation of root hairs in the *etr1-3* and *etr1-7* mutants (Figure 1B). Consistent with our previous results (Harkey et al. 2018), *etr1-3* was less sensitive than Col-0 to the effects of ACC and ethylene, forming fewer and shorter root hairs in the presence of either treatment. The *etr1-7* mutant had larger numbers and longer root hairs in the absence of ACC, although it still responded to ACC and ethylene treatments, suggesting a role for the other ethylene receptors in the formation and elongation of root hairs. Intriguingly, *etr1-7* appeared to be more sensitive to ethylene than to ACC, as only ethylene induced the formation of a dense cluster of root hairs at the root tip under these treatment conditions.

We used our published ACC time-course microarray dataset to determine the best time points for the RNA-Seq analysis (Harkey et al. 2018). We searched for time points that had large numbers of differentially expressed (DE) genes that were not found in other time points and overlapped with the early, middle, and late root hair developmental responses (for details, see Methods). Supplemental Figure 1A displays a pairwise comparison between DE transcripts at each time point. We selected 1 hour as it corresponded to a robust early response and 4 hours as, in our prior experiment, it had 87% of the transcripts that were also DE at 2 hours and 60% of the transcripts that were also DE at 8 hours. This time point is also where ACC began to significantly induce root hair formation (Harkey et al. 2018). This comparison revealed that 1, 4, and 24 hours of ACC treatment yielded large numbers of unique (i.e., not found in other time points) DE transcripts while also overlapping with the root hair developmental responses, so these time points were used in this study.

Principal component analysis and Pearson's correlation reveal patterns among the samples

We performed this RNA-Seq analysis in triplicate with three genotypes (Col-0, *etr1-3*, and *etr1-7*), two treatments (0.75 μM ACC and 0.3 ppm ethylene gas), and four time points (0, 1, 4, and 24 hours). Roots were collected from these samples, and mRNA was isolated and used for RNA-Seq sample preparation. After sequencing and quality control, principal component analysis (PCA) plots were created using 1000 genes with the most variance between samples. Figure 2A shows the PCA plot for all samples, which highlights differences between genotypes across PC1 (*etr1-7*, in particular, is distinct from the other two genotypes), and there is a clear difference across PC2 between ethylene- and ACC-treated samples at time points other than 0. Additionally, one Col-0 control separated from other controls along the vertical axis, which led us to analyze samples within genotypes to further investigate differences between them. These analyses (Supplemental Figure 2; described further in Methods) led us to remove this ethylene time-zero sample as an outlier.

We used the three genotype-specific PCA plots (Figure 2B-D) to assess whether there was variation between the type and duration of treatments. All three plots showed separation of ACC and ethylene samples across the PC1 axis. Meanwhile, the PC2 axis separated samples by time of ethylene or ACC treatment, generally moving from time 0 to time 24 hours from bottom to top. The variation was greater in Col-0 in both PC1 and PC2, consistent with maximal ethylene- and ACC-induced transcriptional responses in Col-0 as opposed to the dampened transcriptional changes in the *etr1-3* mutant due to its reduced ethylene signaling and the *etr1-7* mutant due to its elevated ethylene signaling in the presence and absence of ACC. The diminished response in *etr1-7* was consistent across most of the time points; only the 24-hour time point showed a major change. These patterns suggested that after genotype, treatment accounted for the largest variance among samples followed by treatment duration.

Plots of Pearson's correlation (Figure 2E and Supplemental Figure 3A) and of Euclidean distance (Supplemental Figure 3B and C), with and without hierarchical clustering, were generated to uncover similarities in expression patterns between samples. The scale of the correlation plots suggested that, overall, samples were highly similar, as all correlation values were 0.94 or higher, representing a minimum similarity of 94%. However, some differences were seen in both plots. The *etr1-7* samples tended to cluster primarily with one another, consistent with *etr1-7* having a constitutive transcriptional response to elevated ethylene signaling, while Col-0 and *etr1-3* samples were interspersed with one another, especially in the absence of treatment or at early time points after treatment, consistent with the absence of ethylene responses under those conditions (Figure 2E). To provide additional insight into expression patterns, we also prepared manually arranged plots in which the samples were grouped by genotype, and then the responses to ACC and ethylene were arranged by time within each genotype (Supplemental Figure 3A and B; described further in Methods). These plots also revealed that Col-0 and *etr1-3* showed greater similarity to each other than to *etr1-7*. This separation of *etr1-7* from Col-0 and *etr1-3* was striking, but another pattern also emerged. Replicate 3 of the ethylene-treated samples were consistently different from their matching samples in other replicates, leading to a regular "striping" pattern. This was most obvious in Col-0, slightly less so in *etr1-3*, and although more subtle, also evident in *etr1-7*. This suggested that this third replicate may have had some difference in part of the process such as treatment, sample collection, or sequencing that changed its composition.

We performed ACC treatments at Wake Forest University and ethylene treatments at the University of Tennessee. Therefore, to determine if these samples were similar, we first compared the controls from each location for each genotype, as detailed in Methods. Since the controls for Col-0 and *etr1-3* were well matched between the two locations, and the PCAs suggested

differences in *etr1-7* were not location dependent (Figure 2D), we combined the six untreated (time-0) samples for each genotype, or the five untreated samples for Col-0, excluding the outlier sample described above, to use as the baseline for comparisons for the remaining analyses.

Ethylene treatment stimulated more dramatic transcriptional changes than ACC treatment in Col-0

To summarize how the abundance of transcripts was affected by ethylene and ACC treatment, we first examined the hormone-induced responses in Col-0. For both treatments, every time point was compared back to the same set of combined Col-0 controls, defined above. We created a density plot depicting the number of transcripts as a function of their logFC using those transcripts with a significant adjusted p-value < 0.01 as determined by DESeq2 (Figure 3A). We observed a bimodal distribution at each time point, showing one group of transcripts that increased in abundance and another that decreased in abundance because of these treatments. This pattern was found in response to ethylene and ACC, although there were both larger numbers of DE transcripts and greater magnitude changes in ethylene than in ACC treatment, especially at 1 hour. Both treatments resulted in more down-regulated than up-regulated genes at the 4- and 24-hour time points. The bimodal pattern and higher number of down-regulated genes in response to ACC at the 4- and 24-hour time points were similar to our previous microarray study (Harkey et al. 2018). In contrast, we observed more up-regulated genes in our RNA-Seq study at the 1-hour time point, while the microarray study detected more down-regulated genes at this time point (Harkey et al. 2018). At the 1-hour time point, the bimodal distribution in response to ACC was not observed in the microarray study, likely due to the lower sensitivity of microarrays compared to RNA-Seq, which allows detection of more subtle changes in transcript abundance. In all treatments

and time points, the bimodal distribution representing the increases and decreases in transcript abundance relative to Col-0 at 0 hours were centered on or near -0.5 and 0.5 logFC.

To identify genes with the most robust changes, we utilized a |logFC| > 0.5 and adjusted p-value < 0.01 for the following analyses. Using DESeq2, we identified 4,522 transcripts that were DE using both the logFC and p-value cut offs in response to ethylene and/or ACC in at least one time point in Col-0 (Figure 3B-D). These transcripts and their logFCs (Col-0 treated over Col-0 untreated) are listed in Supplemental File 1. More transcripts responded to ethylene treatment and had a greater logFC than in ACC treatment, though many genes showed similar trends in both treatments: 1,493 and 1,657 genes were down- and up-regulated, respectively, by ethylene only, and 182 and 213 genes were down- and up-regulated, respectively, by ACC only. This logFC cutoff eliminated more genes whose transcripts decreased after treatment, which resulted in a similar number of up- and down-regulated genes passing the logFC cutoff, despite there being more down-regulated genes in the larger set of those with a p-value < 0.01 (Figure 3A). With this cutoff, strikingly, only 16 genes had opposite responses to the two treatments: 3 were down-regulated in ethylene and up-regulated in ACC, and 13 were up-regulated in ethylene and down-regulated in ACC.

This analysis also revealed that 504 and 457 transcripts were up- and down- regulated, respectively, by both ACC and ethylene, whose patterns were shown in Figure 3C and D. One pattern that became apparent was that for transcripts whose abundance decreased after both treatments, the 1- and 24-hour ACC-treated samples did not respond as strongly as the time-matched ethylene-treated samples, while in the 4-hour ACC treatment, the number of transcripts changed more dramatically than time-matched ethylene treatment. This finding suggested the possibility that the rate of conversion of ACC to ethylene resulted in varied ethylene concentrations

across this time course. This pattern of highest absolute logFC at the 4-hour time point was also apparent in the transcripts that were DE only in ACC treatment, and for all transcripts represented in Figure 4.

Transcripts regulated by ethylene and ACC were enriched in functions related to root development

To determine which biological processes were enriched among the transcripts whose abundance changed after ethylene or ACC treatment in Col-0, we performed Gene Ontology (GO) analysis using AgriGO (Du et al. 2010; Tian et al. 2017) and reported the results in Supplemental Table 3. Genes whose transcripts had increased abundance in both treatments were enriched in functional annotations including "negative regulation of the ethylene-mediated signaling pathway," which is consistent with previous findings that both ethylene and ACC transcriptionally regulate components of the ethylene signaling pathway in a negative feedback loop, and response to auxin stimulus, consistent with crosstalk between ethylene and auxin. Several groups of genes, both up- and down-regulated, were enriched in lipid localization and transport annotations.

Transcripts whose abundance decreased in ethylene and/or ACC treatment were enriched in gene annotations including lignin biosynthetic process and cell wall loosening, while transcripts that decreased after only ethylene treatment were enriched in secondary cell wall biogenesis, plant-type cell wall organization, and lignin metabolic process. These results were not surprising given the importance of cell wall remodeling in cell expansion during apical root growth, lateral root emergence, and root hair development.

Interestingly, genes whose transcripts decreased in abundance with ethylene treatment only were enriched in annotations of root hair cell differentiation or root hair development, including

two myosin genes (*XIB* and *XIK*), *MORPHOGENESIS OF ROOT HAIR 1, 2*, and *6*, *ROOT HAIR DEFECTIVE 4* (*RHD4*), *BRISTLED 1*, *CAN OF WORMS 1* (*COW1*), and *SHAVE 2* and *3*. No annotations were significantly enriched in genes down-regulated by ACC only, likely due to the smaller size of this group.

***Transcriptional responses are accentuated in constitutive-signaling* etr1-7 *and reduced in ethylene-insensitive* etr1-3**

We next asked how the transcriptional responses to ethylene and ACC varied in the *etr1-3* and *etr1-7* mutants compared to Col-0. Using a cutoff of |logFC| > 0.5 and adjusted p-value < 0.01, we compared each time point for each treatment and genotype to the Col-0 control and found 8,323 transcripts that were DE in at least one of these genotype comparisons, and these transcripts and their logFCs relative to untreated Col-0 are listed in Supplemental File 1. A heatmap displaying the changes in abundance of these transcripts in all three genotypes and both treatments is shown in Figure 4. All logFC values represented here were relative to Col-0 at time zero to accurately reflect the changes in baseline levels in *etr1-7*.

The heatmap in Figure 4 suggested that the logFC filter eliminated transcripts that responded to ACC, but weaker than to ethylene. As the density plots showed, many transcripts had a |logFC| between 0.25 and 0.5, so we examined transcriptional responses using a less stringent cutoff. When the cutoff was changed to |logFC| > 0.25, we identified 7,104 DE genes in at least one comparison of ethylene and ACC in Col-0, compared to 4,522 with a cutoff of |logFC| > 0.5 (Supplemental Table 3). Regardless of cutoff, the number of transcripts that only responded to ethylene was greater than those only responding to ACC, with approximately 20% of genes

regulated by both ACC and ethylene, 70% by ethylene only, and 10% by ACC only. Therefore, we used the more stringent logFC cutoff of 0.5 for the remaining analyses.

We compared baseline levels of expression in untreated samples between genotypes (Figure 5A), identifying 2,562 genes that were DE (p-value < 0.01) in at least one of these comparisons (these transcripts and their logFCs relative to other genotypes are listed in Supplemental File 2). Consistent with our expectations, *etr1-3* and Col-0 were nearly identical in the absence of elevated ethylene; only 49 out of 2,562 genes were found to be DE between them. However, when we compared *etr1-7* with either Col-0 or *etr1-3*, we found a dramatic difference: 1,941 genes were DE between *etr1-7* and Col-0, and 2,078 genes were DE between *etr1-7* and *etr1-3*. A large number (1,458) of the genes were DE in both comparisons with *etr1-7,* including genes enriched in the "response to ethylene" annotation (Fig. 5B).

One very interesting group of transcripts were the 1,941 transcripts that were DE in *etr1-7* as compared to Col-0, in the absence of hormone treatment. The large number and magnitude change of these genes is consistent with the *etr1-7* mutation being sufficient to lead to large changes in abundances transcripts with endogenous levels of ethylene. Under these conditions, the *etr1-7* mutant has increased root hair formation relative to Col-0. Consistent with this group of genes having an important function in ethylene response, it is enriched in annotations pertaining to the ethylene signaling pathway. Similar annotations were also found in the group of transcripts that responded to ethylene and/or ACC treatment in Col-0, including "response to ethylene" (Supplemental Table 3). These results are consistent with *etr1-7* having constitutive ethylene signaling and therefore a different transcriptional landscape than the other genotypes in the absence of exogenous ethylene or ACC. This group of transcripts is consistent with the *etr1-7* mutation

being sufficient to induce transcript abundance changes that overlap with the treatment of Col-0 with ACC or ethylene.

A subset of ACC- and ethylene-regulated transcript responses appear to be dependent on ETR1 signaling

We developed a more rigorous set of criteria to determine which ethylene- and/or ACC-regulated transcripts were dependent on ETR1 for transcriptional response. For this analysis, we defined a transcript as ETR1-dependent based on the following criteria, with a significant change or response designated as a |logFC| > 0.5 and a p-value < 0.01: 1) transcript showed a significant response to ethylene and/or ACC treatment in at least one time point in Col-0; 2) transcript showed no significant change in any *etr1-3* samples compared to Col-0 time 0; and 3) transcript showed a change in *etr1-7* relative to Col-0 in the baseline and showed similar abundance in ACC- and ethylene-treated *etr1-7* samples. Since *etr1-7* has constitutive ethylene signaling, it should have had transcriptional responses that differed from Col-0 in the absence of either ACC or ethylene treatment and were unchanged by ACC or ethylene treatment. Therefore, we compared *etr1-7* treated samples to *etr1-7* control samples, and only those that did not change with treatment in *etr1-7* qualified as ETR1-dependent.

With this strict criteria, 553 transcripts were identified as ETR1-dependent (listed in Supplemental File 1 with their logFCs relative to untreated Col-0). A subset of 292 transcripts met these criteria in ethylene treatment only, another 191 in ACC only, and 70 genes were classified as ETR1-dependent in both treatments. The heatmap in Figure 6 shows all the transcripts that were ETR1-dependent using these criteria. The logFC values in this table are reported relative to untreated Col-0 samples. It is clear from this heatmap that even though not all of these were DE in

both ACC and ethylene treatments, the difference may simply be tied to a smaller magnitude of ACC response that was below the logFC cutoffs, suggesting that these transcripts are ETR1-dependent regardless of treatment. We also examined the transcripts filtered to have a |logFC| > 0.25, which yielded many more transcripts in each group, but did not change the overall ratios of transcripts in those groups.

Out of the 553 genes which qualified as ETR1-dependent in one or both treatments, 31 overlapped with a set of core ethylene-responsive genes identified by a comparison of three transcriptome studies of ethylene- or ACC-treated roots (Harkey et al. 2018). These genes included *ACC OXIDASE 2* (*ACO2*), *ETHYLENE RESPONSE SENSOR* (*ERS)1* & *2*, and *ETHYLENE AND SALT INDUCIBLE 3* (*ESE3*). This finding suggested there were ETR1-dependent transcriptional responses to ACC and ethylene in this core group. Other ethylene-related genes that did not overlap with this group but were identified as ETR1-dependent here included *ACO3*, several *ERFs*, and *PINOID*, a kinase that is a positive regulator of auxin transport and a negative regulator of root hairs (Lee and Cho 2008). The 553 ETR1-dependent transcripts were enriched in GO annotations including lipid transport, response to ABA, and regulation of transcription (Supplemental Table 4).

We tested an additional set of less stringent criteria, where response to treatment was evaluated by comparing treated samples to the control samples within each genotype, but only required presence or absence of treatment response, regardless of the control sample abundance. In this case, ETR1 dependence was defined by a response in Col-0 but not in the mutants, and ETR1 independence was defined as a response in all three genotypes. This analysis allowed for a larger set of transcripts to be included in both groups (Supplemental Figure 4), but ultimately the changes in abundance of the additional transcripts were not as strong as those seen with the more

stringent criteria, so we focused our analysis on the transcripts that met the more stringent criteria. We continued to calculate, and report in heatmaps, the *etr1-3* and *etr1-7* logFC values relative to Col-0 untreated but used the comparison of *etr1-7* to its own untreated sample for defining ETR1 dependence in the *etr1-7* samples.

Other transcripts appear to be regulated by ACC and/or ethylene in an ETR1-independent manner

Next, we defined ETR1-independent responses for each treatment as having a response to treatment in all genotypes and no altered response in the mutants at baseline (compared to Col-0 time 0). Again, we compared the *etr1-7* treated samples to the *etr1-7* control samples to determine whether a gene responded to treatment in this genotype relative to baseline transcript levels, but in this case a response to treatment was required to qualify as ETR1-independent.

The search for ETR1-independent genes resulted in a slightly smaller set of genes: 481 genes qualified as ETR1-independent in ethylene only, 95 in ACC only, and 117 qualified in both treatments (listed in Supplemental File 1 with their logFCs relative to Col-0 untreated). These ETR1-independent transcripts are shown in the heatmap in Figure 7, where the logFC relative to untreated Col-0 was reported. Unlike the ETR1-dependent genes, these genes showed different patterns depending on whether they met ETR1-independent criteria in ethylene- or ACC-treated samples; genes which were ETR1-independent in one treatment had a reduced response to the other treatment. GO annotations enriched in this group of genes included several stress-response annotations, as well as “root hair cell differentiation” and “unidimensional cell growth” (Supplemental Table 4).

The largest set of genes had complex, but more muted responses to ethylene and/or ACC

After identification of genes with ETR1-dependent and -independent responses, an additional 7,077 genes were left with differential expression in at least one sample (listed in Supplemental File 1 with their logFCs relative to Col-0 untreated). These genes did not meet the strict criteria defined for ETR1-dependent or -independent genes above, showing patterns of response inconsistent with either definition. We divided these "complex" transcripts based on their general patterns across genotypes relative to Col-0 control. A transcript was counted as DE in a genotype if it passed p-value and logFC cutoffs in at least one sample of that genotype as compared to Col-0 control, including control samples for *etr1-3* and *etr1-7* (Supplemental Figure 5). The largest group of genes were those DE in *etr1-7* only (2,974 genes). However, many of these were DE only in one or two samples. The same is true for the 508 and 357 genes which were DE only in Col-0 or *etr1-3*, respectively. The next largest group of 1,068 transcripts had at least one DE sample in each genotype. These transcripts had some response to treatment in all genotypes, so they looked like the ETR1- independent genes but failed the strict filtering used for that group. Similarly, the 1,020 genes that were DE in Col-0 in response to treatment with ACC and/or ethylene and DE between *etr1-7* and Col in the absence of treatment looked like the ETR1-dependent group of genes. Perhaps most puzzling were transcripts which were DE in *etr1-3* and one other genotype, as these did not behave as expected for either ETR1-independent or -dependent genes. In these groups of genes with complex behavior, a wide variety of GO terms were enriched, including response to light stimulus, phenylpropanoid biosynthetic process, response to abscisic acid stimulus, cell wall modification, regulation of transcription, response to ethylene stimulus, and cell wall macromolecule metabolic process (Supplemental Table 4).

Identification of candidates for the ETR1-dependent GRN

Since the ETR1-dependent genes were enriched in the term "regulation of transcription," we asked whether some of these transcripts encoded TFs which may participate in GRNs downstream of ETR1. Using AGRIS (Palaniswamy et al., 2006), we identified 60 ETR1-dependent genes predicted to function as TFs. To prioritize this large group of predicted TFs, we asked which of them were also DE in our ACC microarray dataset (Harkey et al. 2018). We found six TFs that were in the overlap of these datasets (Figure 8). These genes were *RELATED TO AP2 6L* (*RAP2.6L*), *LATERAL ROOT PRIMORDIUM 1* (*LRP1*), *MYB DOMAIN PROTEIN 9* (*MYB9*), *MYB52*, *NAC DOMAIN CONTAINING PROTEIN 58* (*ANAC058*), and *MYB93*. The changes in abundance of these six transcripts over a time course of ACC treatment are shown in Figure 8A. *RAP2.6L* and *LRP1* transcripts exhibited increased abundance over time in response to ACC treatment, while *ANAC058*, *MYB9*, *MYB52,* and *MYB93* transcripts generally decreased in abundance over this time course.

Since ETR1 was previously demonstrated to be the primary receptor controlling the inhibition of lateral root formation and stimulation of root hair initiation in response to elevated ethylene signaling (Harkey et al. 2018), we hypothesized that transcripts that were ETR1-dependent, by our criteria, might also function in repressing lateral root formation or primary root elongation or promoting root hair initiation. We further identified the root cell-type-specific transcript abundance pattern (Brady et al. 2007) for each of these candidate genes and *ETR1* and reported them in a heatmap (Figure 8B). This heatmap showed that *ETR1* had robust levels of expression in pericycle cells, which give rise to lateral roots, and hair cells from which root hairs emerge, consistent with ETR1's role in regulating ethylene-mediated stimulation of root hair growth and inhibition of lateral root formation. The candidate ETR1-dependent genes were also

expressed in lateral roots, pericycle cells, xylem pole pericycle cells, hair cells, and non-hair cells to varying degrees, along with a variety of other root tissue types. Notably, *LRP1* transcripts were highly enriched in lateral root tissue and, to a lesser extent, in pericycle and xylem pole pericycle cells, consistent with LRP1 functioning to regulate lateral root emergence (Singh et al. 2020). *MYB93* transcripts were also highly enriched in xylem pole pericycle cells, consistent with a role for this gene in the inhibition of lateral root formation (Gibbs et al. 2014). For four of these transcripts, there are striking differences in transcript abundance between hair and non-hair cells, with *LRP1* and *MYB9* showing higher abundance in hair cells than non-hair cells, like *ETR1*. In contrast, *ANAC058* and *MYB93* have higher levels in non-hair cells. Interestingly, *MYB52* had low transcript abundance in all root tissues except the maturing xylem. This gene was previously shown to play a role in promoting ABA hypersensitivity, with *MYB52* overexpression lines displaying increased drought tolerance (Park et al. 2011). To illustrate how these genes respond to ethylene and ACC treatment in Col-0, *etr1-3*, and *etr1-7*, we reported the fold change in transcript abundance relative to untreated Col-0 controls for ethylene treatment (Figure 8C-H) and ACC treatment (Supplemental Figure 6). It is clear from these graphs that *LRP1* and *RAP2.6L* transcript levels were induced by ethylene via ETR1, while *ANAC058, MYB9*, *MYB52*, and *MYB93* transcript levels were reduced via this receptor.

ETR1-dependent TF mutants show differences in lateral root formation, root elongation, and root hair initiation

To determine whether these six genes with robust ACC responses encoded TFs that were involved in lateral root formation, we quantified lateral root number in these mutants in the presence and absence of ACC. Briefly, five-day-old seedlings were transferred to plates containing

0 (control) or 0.75 μM ACC and imaged 5 days later. We quantified the number of lateral roots in the region of root that had formed in the absence of ACC and the region of root that was formed after transfer in the presence of ACC, as the inhibition of LR formation by ACC occurs in this region (Negi et al. 2008). We also measured the length of primary root growth and calculated lateral root density in the region of new root growth (see Figure 9C for a diagram of these regions). Representative images of Col-0 and mutant seedlings at 5 days after treatment with ACC (or mock treatment) are shown in Figure 9A (control) and 9B (ACC treated).

We normalized the results to the averages of the Col-0 untreated seedlings for each experiment to both illustrate the extent to which ACC treatment reduced lateral root formation in the mutants and to compare mutant lateral root numbers to Col-0 numbers in the presence and absence of ACC (Figure 9D,E and Supplemental Figure 7) and reported the unnormalized data for all metrics in Supplemental Figure 8. As *etr1-3* (which has reduced ethylene signaling) had higher numbers of lateral roots in the presence and absence of ACC compared to Col-0, and inhibition of lateral root formation by ACC was muted in this genotype (Harkey et al. 2018), we expected mutants in genes that are in the GRN downstream of ETR1 and whose proteins function in the inhibition of lateral root formation by ACC to have phenotypes that looked like *etr1-3* in the presence and absence of ACC. Since *LRP1* and *RAP2.6L* transcripts were both induced over a time course of ACC treatment, we reasoned that the proteins encoded by these genes might function in ACC-mediated inhibition of lateral root formation and therefore the mutants would look like *etr1-3*. Not surprisingly, *lrp1-1* and *rap2.6l-1* mutants both had higher numbers of lateral roots compared to Col-0 in the absence of ACC (Figure 9D). However, only *rap2.6l-1* had higher numbers of lateral roots in the presence of ACC (i.e., muted inhibition of lateral root formation by

ACC). These developmental patterns are consistent with *RAP2.6L* and *LRP1* encoding proteins that function to inhibit lateral root formation.

In contrast to the inhibitory role in lateral root formation of the genes described above, we explored genes whose transcripts decreased in response to ACC treatment, as we thought these might encode proteins that function in the stimulation of lateral root formation, as we would expect the decreased abundance to result in fewer lateral roots. The constitutive-ethylene-signaling mutant *etr1-7* had a reduced number of lateral roots compared to Col-0 in both the presence and absence of ACC (Harkey et al. 2018), and therefore we expected genes that encoded proteins that function to promote lateral root formation to have mutants that looked like *etr1-7* in the presence and absence of ACC. Since *ANAC058*, *MYB9*, *MYB52*, and *MYB93* were downregulated over a time course of ACC treatment (Figure 8B), we speculated that the proteins encoded by these genes might function in the stimulation of lateral root formation. Unexpectedly, we found that *myb9-1* and *myb93-2* had increased numbers of lateral roots compared to Col-0 in the absence of ACC in the region of new root growth, while treatment with ACC brought numbers down to similar levels as Col-0 with ACC treatment (Figure 9D). The increased lateral root number in *myb9-1* in the absence of ACC could be explained by its longer primary roots (Figure 9E), as there was no difference in lateral root density between this mutant and Col-0 (Supplemental Figure 7B). We also observed a similar finding with *myb93-2*, whose lateral root density did not differ from Col-0 in the presence or absence of ACC, although this mutant did not have longer primary roots.

We also compared root elongation in these mutants to Col-0 using both light- and dark-grown seedlings. In light-grown seedlings, the *lrp1-1* and *myb9-1* mutants had longer roots, yet the ability of ACC to inhibit elongation was similar to that observed in Col-0, with other mutants having Col-0 levels of root elongation in the absence of treatment. When these same mutants were

etiolated on ACC (or untreated) plates for 4 days, we found that *lrp1-1* had significantly shorter roots than Col-0 at 0.2 μM ACC, while *myb9-1* behaved like Col-0 at all doses of ACC we tested (Supplemental Figure 9). We also found that *rap2.6l-1*, while its primary roots did not differ from Col-0 when grown under continuous light (Figure 9E), displayed shorter roots at multiple lower doses of ACC (<0.5 μM) after etiolation (Supplemental Figure 9). However, *lrp1-1* and *rap2.6l-1* did not differ from Col-0 at ACC doses of 0.5 μM and higher. For *myb52-1*, this mutant displayed longer roots than Col-0 under control conditions at five days of age (Supplemental Figure 10), although the primary root growth did not differ from Col-0 at ten days of age when lateral roots were measured (Figure 9E). Further, etiolated *myb52-1* seedlings displayed longer roots than Col-0 in the absence of ACC treatment but shorter roots than Col-0 in the presence of 0.2 μM ACC (Supplemental Figure 9). The *anac058-1* mutant was not significantly different from Col-0 at any of the doses of ACC we tested. These results suggested that perhaps some of the candidate genes were more important for light-grown root effects than changes to dark-grown seedlings (Harkey et al. 2019).

We also examined the root hair phenotypes in the six mutants in the presence and absence of ACC. We hypothesized that *RAP2.6L* and *LRP1*, whose transcripts were induced by ACC treatment, to have mutants that looked like *etr1-3* in the presence and absence of ACC, and *ANAC058*, *MYB9*, *MYB52*, and *MYB93*, whose transcripts were downregulated by ACC, to have mutants that looked like *etr1-7* in the presence and absence of ACC. Representative images of the root hair developmental patterns of the 6 mutants were shown in Figure 10A and Supplemental Figure 11A, and quantification of the number of root hairs in the region 0-1,500 μm from the root tip was shown in Figure 10B and 10C and Supplemental Figure 11B. We also reported the raw (unnormalized) values in Supplemental Figure 12A and measurements of the distance to the first

root hair in Supplemental Figure 12B-C. Only *myb52-1* had a statistically significant change in the number of root hairs that formed, with a reduced number of root hairs in both the presence and absence of ACC compared to Col-0 (Figure 10C) and a longer distance to the first root hair (Supplemental Figure 12 C). This is consistent with the absence of a negative regulator of root hair formation, which is reduced in abundance with ACC or ethylene treatment allowing root hairs to form. Consistent with this model, we observed that *myb52-1* had enhanced responsiveness to ACC treatment, as the root hair induction in response to ACC treatment was 2.3-fold in this mutant (compared to 1.5-fold in Col-0).

DAP- and ChIP-Seq data suggested an ETR1-dependent GRN

To better define a GRN downstream of ETR1, we took advantage of publicly available DAP-Seq data, which reported targets of 20% of the TFs in the Arabidopsis genome (O'Malley et al. 2016), and EIN3 ChIP-Seq (Chang et al. 2013) data to reveal TF-target interactions among the 6 ETR1-dependent genes. We found that two of these genes, *LRP1* and *RAP2.6L*, were direct targets of EIN3 in both the DAP-Seq and ChIP-Seq datasets, consistent with the transcripts of these genes being induced by ethylene and ACC treatment (Figure 8).

Of the TFs in our core group of six, the binding sites of only ANAC058 and MYB93 were present in the DAP-Seq dataset. We asked about the enrichment of binding sites for ANAC058 and MYB93 in several of our groups of differentially regulated transcripts to determine where they were most enriched. Among the ETR1-dependent genes, which included these two TFs, ANAC058 and MYB93 were reported to bind to the promoters of 118 (21%) and 139 (25%) of this group of 553 genes, respectively. We also examined the binding events of ANAC058 and MYB93 to the promoters of the larger group of 8,323 genes that were DE in at least one treatment or genotype in

this RNA-Seq dataset, finding that both targeted the promoters of 19% of these genes. Among the ETR1-independent genes, ANAC058 and MYB93 were found to bind to the promoters of 136 (20%) and 122 (18%) of them, respectively. These results are consistent with enrichment of the targets of these genes in the ETR1-dependent group of transcripts.

We examined the TF-target connections among the six candidate genes themselves, using the ANAC058 and MYB93 DAP-Seq data. *ANAC058* was found to be a direct target of MYB93, consistent with *ANAC058* and *MYB93* having similar temporal responses to ACC treatment and being expressed in similar tissue types (Figure 8), while *MYB52* was identified as a direct target of both MYB93 and ANAC058 according to the DAP-Seq data. MYB93 was also found to directly target its own promoter, suggesting the possibility of a positive feedback mechanism with itself. These results, in combination with the phenotype results described above, support a model where *RAP2.6L* encodes a protein that inhibits lateral root formation as a result of EIN3 inducing synthesis of its transcripts. Further, *MYB52* encodes a protein that inhibits root hair initiation in response to ACC, although *MYB52* was not found to be a direct target of EIN3, although under these growth conditions we previously found that *ein3* mutant shows ACC-dependent root development (Harkey et al. 2018). Taken together, the TF-target and phenotype data suggested that the roles of ETR1-dependent genes in root hair initiation and lateral root formation are nuanced and complex with the synthesis of transcripts for some genes requiring EIN3 directly while others may function independently of EIN3.

Discussion

The Arabidopsis genome encodes five ethylene receptors that have distinct and overlapping functions in the regulation of plant growth, with the role of individual receptors in ethylene-

regulated development described only in several tissues (Binder 2020; Cancel and Larsen 2002; Ma and Dong 2021). These receptors negatively regulate the ethylene signaling pathway and are turned off by the binding of ethylene, inducing downstream changes in transcription. In roots, ETR1 is the receptor that is most strongly linked to the inhibition of lateral root formation and primary root elongation and the stimulation of root hair growth by ACC (Harkey et al. 2018). To understand the regulatory mechanisms by which ETR1 controls these processes, we identified genome-wide changes in transcript abundance in roots in response to treatment with ethylene or its precursor, ACC, using Col-0 and LOF and GOF *etr1* receptor mutants, providing new candidate genes that may drive these root developmental processes downstream of ETR1.

We began by examining the transcriptional response of Col-0 to ethylene and ACC to determine similarities and differences in the transcriptional responses. We identified doses of ethylene and ACC that had similar root developmental responses and quantified changes in transcript abundance in response to ethylene and ACC treatment at 3 times of treatment. We identified DE transcripts and the direction and magnitude change of abundance of these transcripts in response to elevated levels of ethylene or ACC. Ethylene induced a greater number of DE genes than ACC at all time points after treatment with larger magnitude changes in transcript abundance. The most likely explanation for this result was that ethylene gas used in our treatments elevated ethylene to levels higher than the levels of ethylene produced from conversion of ACC.

Several reports have suggested that ACC may act as a signal independently of its conversion to ethylene, especially at high concentrations where ACO-dependent conversion becomes rate limiting (Houben and Van de Poel 2019). At concentrations of 10 µM and above, ACC inhibits rosette size and growth across all tissues in seedlings (Vanderstraeten et al. 2019). However, roots of the ethylene-insensitive *ein2-1* and *ein2-5* mutants do not respond to 1 µM ACC

(Harkey et al. 2018; Ivanchenko et al. 2008; Muday et al. 2012; Negi et al. 2008; Růžička et al. 2007), suggesting that ACC is either completely converted to ethylene or does not control development independent of its conversion to ethylene in these tissues under these treatment and growth conditions. Our finding that most of the genes that were DE in response to ACC were also DE in response to ethylene is consistent with that possibility. There were only 395 genes, or 9% of all ethylene- and/or ACC-regulated genes, that were DE in response to ACC only, consistent with the conversion of ACC to ethylene at this dose and minimal direct or distinct effects of ACC eliciting significant transcriptional responses independently of ethylene. The differences in the magnitude of transcript abundance changes between the treatments were likely due to limitations in cellular uptake of ACC and the additional step required to convert ACC to ethylene by ACO (Houben and Van de Poel 2019), resulting in less and delayed ethylene signaling in the ACC-treated seedlings than in seedlings directly treated with ethylene gas. It is also worth noting that in both treatments the majority of transcriptional changes were negative, especially at the 4- and 24-hour time points. This observation is in alignment with our previous observation that ACC treatment induced more negative changes in transcript abundance than positive ones (Harkey et al. 2018).

We identified ETR1-regulated genes using two *etr1* mutant alleles: *etr1-3*, which is a gain-of-function (GOF) receptor mutant with a constitutively active receptor that turns off ethylene signaling, resulting in an ethylene-insensitive phenotype, and *etr1-7*, which is a loss-of-function (LOF) receptor mutant that has an inactive receptor, resulting in constitutive ethylene signaling. The combination of using GOF and LOF receptor mutants served as a powerful approach to identify ETR1-dependent transcriptional responses. This is clear from the earliest steps of the analysis; a PCA plot comparing all samples led to the separation of *etr1-7* samples from Col-0 and

etr1-3 on the PC1 axis (Figure 2A). This pattern was also observed in the Pearson's correlation and Euclidean distance plots, which showed that *etr1-7* samples were more like each other than either Col-0 or *etr1-3* (Figure 2E and Supplemental Figure 3). When we examined genes which were DE when comparing the genotype control samples to each other, most genes were found DE in comparisons of *etr1-7* to Col-0 or *etr1-3*. In contrast, in the absence of ACC or ethylene, Col-0 and *etr1-3* had nearly identical transcriptional profiles (Figure 5). In a heatmap of all transcripts that changed in Col-0 and the *etr1* mutants in response to ACC and/or ethylene (Figure 4), many of the transcripts that changed in *etr1-7* had transcript abundances that changed in the same direction upon ACC or ethylene treatment. Together, these data demonstrated the dramatic effect that constitutive signaling through ETR1 had on the transcriptional profile of Arabidopsis.

We compared the transcriptional profiles of these mutants to Col-0 in the presence and absence of ethylene or ACC to identify transcripts whose changes in abundance were tied to ETR1 functionality. The criteria by which we determined whether a gene was ETR1 dependent were the following: 1) if it had a significant change in response to ethylene and/or ACC treatment in at least one time point in Col-0; 2) if it showed no significant change in all treatment samples in *etr1-3* compared to Col-0 time 0; and 3) if it showed a significant change in *etr1-7* relative to Col-0 in the baseline with no further changes across the time points. We organized transcripts by their responses, classifying them as ETR1-dependent, ETR1-independent, or complex. ETR1-dependency was defined using stringent criteria to identify only genes which clearly required this receptor for transcriptional response to ACC or ethylene. The strict ETR1-dependent group was enriched in the "ethylene mediated signaling pathway" annotation, and the complex genes that failed to meet our strict criteria for ETR1 dependency or independency (but included putatively ETR1-dependent genes) were enriched in the "response to ethylene stimulus" annotation.

We previously identified a group of core ethylene-responsive genes in roots, created by comparing transcriptome data from plants treated with ethylene or ACC under growth conditions that varied by light duration, from darkness to 24-hour light (Harkey et al. 2019). We compared this list with the ETR1-dependent responses. Genes that were in the core group and were found here to be ETR1-dependent included *ETHYLENE AND SALT INDUCIBLE 3 (ESE3)*, as well as ethylene receptors *ERS1* and *ERS2*; we previously showed via RT-qPCR that *ERS1* and *ERS2* were not induced in the *etr1-3* mutant (Harkey et al. 2018). Genes that were complex and appeared ETR1-dependent (but failed the strict criteria used to define that group) and were found in the group of core ethylene-responsive genes in roots included *REVERSION TO ETHYLENE SENSITIVITY 1* (*RTE1*) and the transcription factor *NAM*, which we recently showed to be involved in ethylene-regulated primary root and lateral root formation (Harkey et al. 2020). These putatively ETR1-dependent genes were also enriched in sucrose signaling, which is known to be involved in root elongation (Kircher and Schopfer 2012).

To identify the GRN downstream of ETR1 controlling root responses to ethylene, we overlapped the list of ETR1-dependent genes with an ACC microarray dataset that identified genes with robust responses to elevated ethylene signaling over a time course (Harkey et al. 2018), identifying six genes predicted to encode TFs. These genes were *LATERAL ROOT PRIMORDIUM 1 (LRP1), MYB DOMAIN PROTEIN 9 (MYB9), MYB52, MYB93, NAC DOMAIN CONTAINING PROTEIN 58 (ANAC058)*, and *RELATED TO AP2 6L (RAP2.6L)*. In the microarray dataset, transcript abundance of *LRP1* and *RAP2.6L* increased over time, while transcript abundance of *MYB9*, *MYB52*, *MYB93*, and *RAP2.6L* decreased over time in response to exogenous ACC.

All these transcripts were detected in at least one of the following tissue types in roots: lateral roots, pericycle (including the xylem pole pericycle), hair cells, and non-hair cells. *ETR1*

transcripts were highly enriched in pericycle and hair cells, consistent with its role in modulating lateral root and root hair formation. We examined these candidate ETR1-dependent genes to determine if they had alterations in formation of root hairs or lateral roots or primary root elongation in the presence and absence of ACC. We found that *lrp1-1*, *myb9-1*, *myb93-2* and *rap2.6l-1* all had increased lateral root numbers in the region of new root growth in the absence of ACC, which suggested that *LRP1*, *MYB9*, *MYB93*, and *RAP2.6L* encoded proteins that functioned to repress lateral root formation. In alignment with these findings, we observed enrichment of *LRP1* and *MYB93* transcripts in lateral roots and xylem pole pericycle cells, respectively, while all four genes were expressed in tissues that give rise to lateral roots.

We compared lateral root development in these mutants to reports in the literature. One study found that overexpression of *LRP1* resulted in an increased number of lateral root primordia and a reduced number of emerged lateral roots (Singh et al. 2020), which was consistent with the *lrp1-1* mutant having more emerged lateral roots than Col-0. Consistent with our *myb93-2* results, another study found that a different *myb93* allele, *myb93-1*, also had more lateral roots than Col-0 (Gibbs et al. 2014). For *RAP2.6L*, one study found that overexpression of this gene resulted in significant inhibition of adventitious root initiation but did not have an effect on lateral root number or density (Lakehal et al. 2020). In contrast, we found that the *rap2.6l-1* mutant had more lateral roots compared to Col-0 in both the presence and absence of ACC, suggesting a role for RAP2.6L in the inhibition of lateral root formation by ethylene signaling. An explanation for this contradictory finding could be that overexpressing RAP2.6L may not have an effect in tissues where it is already expressed. Further, these differences could be due to differences in plant media or light conditions.

We also examined several other phenotypes: root hair formation and primary root elongation in light and dark grown seedlings. We found that the *myb52-1* mutant had reduced root hair numbers in both the presence and absence of ACC, although there was enhanced induction in root hair initiation by ACC in this mutant compared to Col-0, suggesting that MYB52 functions to inhibit root hair initiation by ethylene signaling. This finding was consistent with published data showing that MYB52 functions as a positive regulator of ABA signaling, which represses root hair growth in Arabidopsis (Park et al. 2011).

Using publicly available TF-target data, *RAP2.6L* and *LRP1* were found to be direct targets of EIN3, consistent with transcription of these genes being induced by ethylene. *MYB52* was found to be a direct target of both ANAC058 and MYB93, while, interestingly, MYB93 also bound to its own promoter, indicative of self-regulation. The direct interactions among these genes were consistent with these genes all being down-regulated by ethylene. Together, the phenotype results in combination with the TF-target data suggest complex roles of the ETR1-dependent genes in root development.

An unexpected finding in this study was that there were nearly as many transcripts that responded in an ETR1-independent fashion as those that were ETR1-dependent. Transcripts were defined as ETR1-independent if they responded to treatment in all three genotypes. Complex genes were putatively ETR1-independent if they had at least one DE sample in at least one genotype (relative to Col-0 time 0 for Col-0 and *etr1-3* treated samples or relative to *etr1-7* time 0 for *etr1-7* treated samples) but did not show consistent response across all three genotypes. A total of 693 and 1,068 transcripts met these criteria (ETR1-independent and putatively ETR1-independent, respectively). These numbers were very similar to the number of transcripts that qualified as ETR1-dependent or nearly so (553 and 1,020). This finding was surprising given the importance

of ETR1 for root developmental responses, but perhaps these ETR1-independent transcripts could be split into two groups: those that mediated ETR1-independent developmental responses, and those which did not directly affect the phenotypes we have measured.

In our prior study we found ETR1 to be essential in some root developmental responses and identified roles for other ethylene receptors in other responses. ACC effects on lateral root development were completely lost in the ethylene-insensitive mutant *etr1-3* and not induced by addition of ACC in the constitutively signaling mutant *etr1-7*, suggesting inhibition of lateral root formation by ethylene signaling had strong dependence on ETR1. In contrast, inhibition of primary root elongation and stimulation of root hair growth by ACC were less dependent on ETR1 as they showed attenuated responses to ACC in *etr1-7* (Harkey et al. 2018), suggesting the role of other ethylene receptors in these root processes. Perhaps some of the transcripts which were ETR1 independent were involved in root elongation or root hair initiation. Indeed, when we examined genes that were ETR1-independent by the strictest criteria, they were enriched in the annotation "root hair cell differentiation" and several other related annotations. Complex genes which included those that were putatively ETR1-independent included annotations for "cell wall modification" and "plant-type cell wall organization," so these genes may also be involved in polar tip expansion to drive root hair formation or cell elongation to drive primary root growth or emergence of lateral roots.

We also compared the two groups of strictly and partially ETR1-independent genes to the set of core ethylene-responsive genes in roots (Harkey et al. 2019). Genes which were strictly ETR1-independent and in the core group included *ERF73*, while the overlap of the core group and partially ETR1-independent genes included *ACO1*, *EIN3-BINDING F BOX PROTEIN 2* (*EBF2*), *ETHYLENE RESPONSE DNA BINDING FACTOR 3* (*EDF3*), two expansins (*EXP12* and

EXPB1), and *ETR2*, the remaining of the three ethylene receptors known to be induced by ethylene (Harkey et al. 2018). If these genes were truly ETR1-independent, it is likely that ETR2 or EIN4 were responsible for their changes in transcript abundance. Beyond transcriptional changes which lead to visible effects on root development, it is likely that some ETR1-independent responses were also responsible for changes in primary or specialized metabolism.

We demonstrated here that in Arabidopsis roots, low levels of ACC do not have a significant effect on transcription outside of responses induced by ethylene application. We differentiated transcriptional responses which required the receptor ETR1, and those that functioned through other parts of the ethylene signaling pathway, presumably through ETR2 and EIN4. We performed functional analysis using mutants and identified ETR1-dependent genes that functioned in the inhibition of lateral root formation or stimulation of root hair initiation by ACC. This dataset contains a wealth of information which can be mined to further understand the transcriptional response networks by which ethylene controls Arabidopsis root development.

Methods

Genotypes and plant growth conditions

All mutants used in this study were in the Col-0 background. Both the *etr1-3* and *etr1-7* alleles have been described previously (Guzmán and Ecker 1990; Harkey et al. 2018; Hua and Meyerowitz 1998). The *etr1-7* (AT1G66340) mutant was obtained from Elliot Meyerowitz (Hua and Meyerowitz 1998). T-DNA insertion mutants were obtained from the Arabidopsis Biological Resource Center for AT3G18400 (SALK_049205C), AT5G12330 (SAIL_402_G06/CS873836), AT5G16770 (SALK_149765C), AT1G17950 (SALK_138624C), AT1G34670 (GK_588A05),

and AT5G13330 (SALK_051006C); see Supplemental Table 5 for more information on these lines.

Plants were grown on 1× Murashige and Skoog medium (Caisson Laboratories), pH 5.6, Murashige and Skoog vitamins, and 0.8% agar, buffered with 0.05% MES (Sigma), and supplemented with 1% sucrose. After stratification for 72 h at 4°C, plants were grown under 100-130 µmol m^{-2} s^{-1} continuous cool-white light.

For selecting a dose of ethylene for the RNA-Seq, Col-0 seedlings were treated on day 5 after germination. For ACC treatment, the seedlings were transferred to a growth medium containing 0 or 0.75 µM ACC for 24 hours before imaging. For ethylene treatment, plates were placed in clear treatment tanks with constant flow-through of the indicated concentration of ethylene for 24 hours before imaging.

Method for selecting time points for RNA-Seq analysis using a previous microarray study

We developed an analysis approach to identify the subset of time points that contained the most unique (i.e., not found in other time points) DE genes in response to ACC treatment using our previously published time-course microarray study with ACC treated Col-0 roots (Harkey et al. 2018). In that prior study, we examined transcriptional responses to 1 µM ACC after 0.5, 1, 2, 4, 8, 12, and 24 hours of treatment, which overlaid the timeline for ACC-induced root hair initiation. To inform the selection of time points for the present study, we used the microarray data t. We first analyzed the microarray data to find DE genes for each individual time point compared to time zero. We then performed a pairwise comparison of time points to determine the number of overlapping DE genes between each time point (Supplemental Figure 1B) and the percent of DE genes in a time point that overlapped with another time point (Supplemental Figure 1A). These

results revealed that treatment times of 1, 4, and 24 hours contained the most unique sets of transcripts while also overlapping with the timing of root hair formation to capture early, middle, and late developmental responses. Therefore, we chose to perform RNA-Seq using samples treated with ACC or ethylene at 3 time points: 1 hour, to monitor rapid transcriptional responses that precede developmental changes; 4 hours, where the most unique transcripts are DE and root hair initiation and primary root elongation are increasing and decreasing, respectively, in response to treatment; and 24 hours to identify transcripts linked to ethylene-modulated lateral root regulation.

Microarray data (Harkey et al. 2018) was analyzed using limma (Ritchie et al. 2015). Probes were first filtered for interquartile range (IQR), with anything less than 0.1 excluded from further analysis. Time points were then compared to their time-matched controls; p-values were adjusted using a Benjamini-Hochberg correction. Genes with an |logFC| greater than 0.5 and an adjusted p-value less than 0.05 were DE at that time point. The overlap matrix was created by comparing the DE genes across the time points in a pair-wise manner.

Supplemental Figure 1A graphically illustrates the results of this analysis. For each column, the percentage of DE genes at that time point (column) that are also DE in the time point to which it was compared (row) is shown. The number of genes in each comparison that was used to calculate the percentages can be seen in Supplemental Figure 1B. For example, the 2-hour time point showed considerable overlap with the 4-hour time point; 87% of all 2-hour DE genes were also DE at 4 hours. The reverse comparison of the 4-hour genes that were also DE at 2 hours yielded only 32% of the 4-hour genes that were DE at 2 hours because there were more DE genes in this 4 hour sample. Therefore, the 4-hour time point identified nearly all the same DE genes as the 2-hour time point, as well as many more unique genes, so we selected the 4-hour time point over the 2-hour for this RNA-Seq analysis. We also examined the overlaps of the 4- and 8-hour

time points and the 12- and 24-hour time points, finding more unique DE transcripts in the 8- and 24-hour time points for each of these overlaps. However, as root hairs had already begun to initiate by 4 hours (Harkey et al. 2018), and the ethylene-dependent inhibition of lateral root initiation had begun by 24 hours, these time points also represented important developmental milestones. Ultimately, this analysis informed our choice to do the present experiment with time points 0, 1, 4, and 24 hours.

ACC and ethylene treatment of seedlings for RNA isolation for sequencing

Plants were grown on media as described above on top of a nylon filter (03-100/32; Sefar Filtration) pressed against the plate, as described previously (Harkey et al. 2018; Levesque et al. 2006). Approximately 100 sterilized seeds were placed on each filter; 2 plates were combined for each biological replicate. ACC-treated samples were grown and harvested at Wake Forest University and ethylene-treated samples were grown and harvested at the University of Tennessee Knoxville utilizing a gas flow-through system to treat with constant levels of ethylene gas. The same researchers prepared both sets of samples and identical reagents and light treatments were used in both laboratories. Time 0 controls were prepared in both locations to account for any location-specific effects on baseline expression.

Plants were treated on day 5 after germination. For time 0 treatments, the nylon filter containing 5-day-old plants was transferred to new control medium and root tissue was immediately harvested. For ACC treatment, the plants on nylon were transferred to growth medium with 1 μM ACC for the given treatment time (1, 4, and 24 h) and then root tissue was harvested. For ethylene treatment, the nylon was transferred to new control medium, and plants were placed in clear treatment tanks with constant flow-through of 0.3 ppm ethylene gas for the

given treatment time (1, 4, and 24 h) and then root tissue was harvested. At time of harvesting, roots were cut from seedlings and flash frozen in liquid nitrogen. Frozen samples were ground in liquid nitrogen, and RNA isolation was performed according to the Qiagen plant RNeasy kit protocol, with the addition of the Qiagen RNase-free DNase treatment (Qiagen). After RNA isolation, samples were quantified by A260 using a Nanodrop spectrophotometer (Nanodrop Technologies). Each sample yielded at least 3 µg, and on average 15 µg, of RNA. One Col-0 sample which had a 4-hour ethylene treatment had an RNA integrity number (RIN) less than 6 and was not sequenced. Sequencing was performed by GENEWIZ, LLC using the Illumina HiSeq platform.

RNA-Seq preprocessing and quality control

FastQC v0.11.8 (Wingett and Andrews 2018) and MultiQC v1.7 (Ewels et al. 2016) were used for assessing read quality, which identified adaptor contamination and a bimodal GC Content distribution. Adaptors were trimmed from reads using CutAdapt v1.18 (Martin 2011), and reads trimmed to less than 25 bp were removed. Trimmed reads were then processed with the BBMap tool BBDuk (Bushnell 2014) to identify and remove rRNA contamination. Running FastQC/MultiQC over the trimmed and filtered reads revealed the identified quality issues had been mitigated. Read quantification was performed directly on the processed fastq files with the Salmon v0.12.0 (Patro et al. 2017) "quant" algorithm in mapping mode using the "--validateMapping" flag, setting the library type to "IU", and using the TAIR10 reference transcriptome (NCBI ID: GCF_000001735.3). Counts were imported into R v3.6.0 using the tximport R package v1.12.3 (Soneson et al. 2016) and summarized to the gene level.

Differential expression and visualization

For visualization and sample comparisons, raw read counts were normalized using the Variant Stabilizing Transformation method from the R package DESeq2 v1.24.0 (Love, Huber, and Anders 2014). Sample-wise comparison heatmaps were generated using Pearson's correlation and Euclidean distance as the distance metrics, respectively. PCA analyses were performed by DESeq2's plotPCA method using the top 1000 most variable genes for all genotypes together, and on a per-genotype basis.

All sample-wise comparisons were performed using the DESeq2 package and ashr v2.2-47 (Stephens et al. 2020). Density plots were generated using ggplot2 v3.3.0 (Wickham 2016), and heatmaps of sample-wise comparisons were generated using ComplexHeatmap v.2.3.4 (Gu et al. 2016). For DE transcripts used in heatmaps and GO analyses, we considered a transcript to be DE if it had a p-value < 0.01, $|\text{logFC}| > 0.5$, and baseMean > 10.

Method to identify and remove outlier control sample

To determine if all the control samples could be pooled for calculation of logFC of samples, we generated a PCA plot using only the Col-0 samples (Supplemental Figure 2). This revealed that one control (an ethylene time 0 sample) did not cluster with the 5 other control samples. This single sample showed separation on the PC1 axis, which represents over 50% of the variance across all the Col-0 samples. This sample was found to have far lower RNA yield than the other 71 samples prepared. This analysis suggested that this sample should be removed from the rest of our analyses. We generated a new PCA plot without it present revealing much great consistency.

To further validate this method, we performed a differential expression analysis to look for differences in transcripts between locations with all six Col-0 control samples (three from each

location) and with the outlier sample removed. When all 6 samples were included, 693 genes were found to be DE between the ACC and ethylene controls performed at these two locations (Supplemental Table 1, adjusted p-value < 0.01, |logFC| > 0.5). When the outlier sample identified by the PCA plot was removed from the analysis, only 34 genes were found to be DE between the Col-0 samples. This removal also affected the model generated by DESeq2, resulting in subtle effects on the *etr1-3* and *etr1-7* comparisons. In the model with the outlier Col-0 removed, 121 and 763 genes were DE between the controls compared at each location in *etr1-3* and *etr1-7*, respectively. The *etr1-7* time 0 samples had more DE genes than was expected, but there were two controls that were quite different than other samples (as evident in the PCA analysis in Figure 2D), which suggested that this is a character of 2 samples rather than a difference in samples because of location. We ultimately decided to combine the control samples for each genotype from both locations.

PCR genotyping

The primers used for genotyping are reported in Supplemental Table 5. Young leaf tissue was homogenized in a microcentrifuge tube using a micropestle that was dipped in liquid nitrogen. Edwards Solution (Edwards, Johnstone, and Thompson 1991) was added to the homogenized leaf tissue and samples were incubated at room temperature for at least one hour before being spun down. Supernatant was carefully transferred to a new tube containing an equal volume of isopropanol. Samples were washed with EtOH and air dried in a sterile hood for approximately 30 minutes before being resuspended in molecular biology grade H_2O. Genotype was determined using wild-type primers that flanked the T-DNA insert (the wild-type reaction) to amplify the gene, and right border primers with T-DNA primers (the T-DNA reaction) to amplify the T-DNA insert (O'Malley, Barragan, and Ecker 2015), with primer sequences listed in Supplemental Table 5.

DreamTaq DNA Polymerase (ThermoFisher) was used according to the manufacturer's instructions.

Root development analysis

For analysis of root hair and lateral root phenotypes, five-day-old seedlings were transferred to plates containing 0 or 0.75 μM ACC for 4 hours or 5 days before imaging root hairs and lateral roots, respectively. For the root length analysis of dark grown seedlings, seeds were germinated in the dark for 4 days on untreated plates or plates containing 0.1, 0.2, 0.5, 1 or 2 μM ACC, then root lengths were measured. Statistical tests (two-way ANOVA and multiple comparisons tests) were performed in GraphPad Prism 8.0.2. Outliers were identified using ROUT (Q = 1%).

Acknowledgements

This work was supported by the National Science Foundation Systems and Synthetic Biology (MCB-1716279 to GKM) and the Center for Molecular Signaling Graduate Research Fellowship to MGK.

References

Abeles, Frederick B., Page W. Morgan, and Mikal E. Saltveit. 1992. *Ethylene in Plant Biology*. 2nd ed. San Diego: Academic Press.

Alonso, Jose M., Takashi Hirayama, Gregg Roman, Saeid Nourizadeh, and Joseph R. Ecker. 1999. "EIN2, a Bifunctional Transducer of Ethylene and Stress Responses in Arabidopsis." *Science* 284(5423):2148–52. doi: 10.1126/science.284.5423.2148.

Alonso, Jose M., and Anna N. Stepanova. 2004. "The Ethylene Signaling Pathway." *Science* 306(5701):1513–15. doi: 10.1126/science.1104812.

An, Fengying, Qiong Zhao, Yusi Ji, Wenyang Li, Zhiqiang Jiang, Xiangchun Yu, Chen Zhang, Ying Han, Wenrong He, Yidong Liu, Shuqun Zhang, Joseph R. Ecker, and Hongwei Guo. 2010. "Ethylene-Induced Stabilization of ETHYLENE INSENSITIVE3 and EIN3-LIKE1 Is Mediated by Proteasomal Degradation of EIN3 Binding F-Box 1 and 2 That Requires EIN2 in Arabidopsis." *The Plant Cell* 22(7):2384–2401. doi: 10.1105/tpc.110.076588.

Berleth, Mareike, Niklas Berleth, Alexander Minges, Sebastian Hänsch, Rebecca Corinna Burkart, Björn Stork, Yvonne Stahl, Stefanie Weidtkamp-Peters, Rüdiger Simon, and Georg Groth. 2019. "Molecular Analysis of Protein-Protein Interactions in the Ethylene Pathway in the Different Ethylene Receptor Subfamilies." *Frontiers in Plant Science* 10.

Binder, Brad M. 2020. "Ethylene Signaling in Plants." *Journal of Biological Chemistry* 295(22):7710–25. doi: 10.1074/jbc.REV120.010854.

Binder, Brad M., Ronan C. O'Malley, Wuyi Wang, Tobias C. Zutz, and Anthony B. Bleecker. 2006. "Ethylene Stimulates Nutations That Are Dependent on the ETR1 Receptor." *Plant Physiology* 142(4):1690–1700. doi: 10.1104/pp.106.087858.

Brady, Siobhan M., David A. Orlando, Ji-Young Lee, Jean Y. Wang, Koch, José R. Dinneny, Daniel Mace, Uwe Ohler, and Philip N. Benfey. 2007. "A High-Resolution Root Spatiotemporal Map Reveals Dominant Expression Patterns." *Science* 318(5851):801–6. doi: 10.1126/science.1146265.

Bushnell, Brian. 2014. "BBMap: A Fast, Accurate, Splice-Aware Aligner." doi: https://escholarship.org/uc/item/1h3515gn.

Cancel, Jesse D., and Paul B. Larsen. 2002. "Loss-of-Function Mutations in the Ethylene ReceptorETR1 Cause Enhanced Sensitivity and Exaggerated Response to Ethylene in Arabidopsis." *Plant Physiology* 129(4):1557–67. doi: 10.1104/pp.003780.

Chang, Caren, Shing F. Kwok, Anthony B. Bleecker, and Elliot M. Meyerowitz. 1993. "Arabidopsis Ethylene-Response Gene ETR1: Similarity of Product to Two-Component Regulators." *Science* 262(5133):539–44. doi: 10.1126/science.8211181.

Chang, Katherine Noelani, Shan Zhong, Matthew T. Weirauch, Gary Hon, Mattia Pelizzola, Hai Li, Shao-shan Carol Huang, Robert J. Schmitz, Mark A. Urich, Dwight Kuo, Joseph R. Nery, Hong Qiao, Ally Yang, Abdullah Jamali, Huaming Chen, Trey Ideker, Bing Ren, Ziv Bar-Joseph, Timothy R. Hughes, and Joseph R. Ecker. 2013. "Temporal Transcriptional Response to Ethylene Gas Drives Growth Hormone Cross-Regulation in Arabidopsis" edited by D. Weigel. *eLife* 2:e00675. doi: 10.7554/eLife.00675.

Dolgikh, Vladislav A., Evgeniya M. Pukhovaya, and Elena V. Zemlyanskaya. 2019. "Shaping Ethylene Response: The Role of EIN3/EIL1 Transcription Factors." *Frontiers in Plant Science* 10.

Du, Zhou, Xin Zhou, Yi Ling, Zhenhai Zhang, and Zhen Su. 2010. "agriGO: A GO Analysis Toolkit for the Agricultural Community." *Nucleic Acids Research* 38(suppl_2):W64–70. doi: 10.1093/nar/gkq310.

Edwards, K., C. Johnstone, and C. Thompson. 1991. "A Simple and Rapid Method for the Preparation of Plant Genomic DNA for PCR Analysis." *Nucleic Acids Research* 19(6):1349–1349. doi: 10.1093/nar/19.6.1349.

Ewels, Philip, Måns Magnusson, Sverker Lundin, and Max Käller. 2016. "MultiQC: Summarize Analysis Results for Multiple Tools and Samples in a Single Report." *Bioinformatics* 32(19):3047–48. doi:

10.1093/bioinformatics/btw354.
Feng, Ying, Ping Xu, Bosheng Li, Pengpeng Li, Xing Wen, Fengying An, Yan Gong, Yi Xin, Ziqiang Zhu, Yichuan Wang, and Hongwei Guo. 2017. "Ethylene Promotes Root Hair Growth through Coordinated EIN3/EIL1 and RHD6/RSL1 Activity in Arabidopsis." *Proceedings of the National Academy of Sciences* 114(52):13834–39. doi: 10.1073/pnas.1711723115.
Ge, Steven Xijin, Dongmin Jung, and Runan Yao. 2020. "ShinyGO: A Graphical Gene-Set Enrichment Tool for Animals and Plants." *Bioinformatics* 36(8):2628–29. doi: 10.1093/bioinformatics/btz931.
Gibbs, Daniel J., Ute Voß, Susan A. Harding, Jessica Fannon, Laura A. Moody, Erika Yamada, Kamal Swarup, Candida Nibau, George W. Bassel, Anushree Choudhary, Julien Lavenus, Susan J. Bradshaw, Dov J. Stekel, Malcolm J. Bennett, and Juliet C. Coates. 2014. "AtMYB93 Is a Novel Negative Regulator of Lateral Root Development in Arabidopsis." *New Phytologist* 203(4):1194–1207. doi: 10.1111/nph.12879.
Gu, Zuguang, Roland Eils, and Matthias Schlesner. 2016. "Complex Heatmaps Reveal Patterns and Correlations in Multidimensional Genomic Data." *Bioinformatics* 32(18):2847–49. doi: 10.1093/bioinformatics/btw313.
Guzmán, P., and J. R. Ecker. 1990. "Exploiting the Triple Response of Arabidopsis to Identify Ethylene-Related Mutants." *The Plant Cell* 2(6):513–23. doi: 10.1105/tpc.2.6.513.
Harkey, Alexandria F., Kira N. Sims, and Gloria K. Muday. 2020. "A New Tool for Discovering Transcriptional Regulators of Co-Expressed Genes Predicts Gene Regulatory Networks That Mediate Ethylene-Controlled Root Development." *In Silico Plants* 2(1):diaa006. doi: 10.1093/insilicoplants/diaa006.
Harkey, Alexandria F., Justin M. Watkins, Amy L. Olex, Kathleen T. DiNapoli, Daniel R. Lewis, Jacquelyn S. Fetrow, Brad M. Binder, and Gloria K. Muday. 2018. "Identification of Transcriptional and Receptor Networks That Control Root Responses to Ethylene." *Plant Physiology* 176(3):2095–2118. doi: 10.1104/pp.17.00907.
Harkey, Alexandria F., Gyeong Mee Yoon, Dong Hye Seo, Alison DeLong, and Gloria K. Muday. 2019. "Light Modulates Ethylene Synthesis, Signaling, and Downstream Transcriptional Networks to Control Plant Development." *Frontiers in Plant Science* 10.
Houben, Maarten, and Bram Van de Poel. 2019. "1-Aminocyclopropane-1-Carboxylic Acid Oxidase (ACO): The Enzyme That Makes the Plant Hormone Ethylene." *Frontiers in Plant Science* 10.
Hua, Jian, and Elliot M. Meyerowitz. 1998. "Ethylene Responses Are Negatively Regulated by a Receptor Gene Family in Arabidopsis Thaliana." *Cell* 94(2):261–71. doi: 10.1016/S0092-8674(00)81425-7.
Hua, Jian, Hajime Sakai, Saeid Nourizadeh, Qianhong G. Chen, Anthony B. Bleecker, Joseph R. Ecker, and Elliot M. Meyerowitz. 1998. "EIN4 and ERS2 Are Members of the Putative Ethylene Receptor Gene Family in Arabidopsis." *The Plant Cell* 10(8):1321–32. doi: 10.1105/tpc.10.8.1321.
Huang, Yafan, Hui Li, Claire E. Hutchison, James Laskey, and Joseph J. Kieber. 2003. "Biochemical and Functional Analysis of CTR1, a Protein Kinase That Negatively Regulates Ethylene Signaling in Arabidopsis." *The Plant Journal* 33(2):221–33. doi: 10.1046/j.1365-313X.2003.01620.x.
Ivanchenko, Maria G., Gloria K. Muday, and Joseph G. Dubrovsky. 2008. "Ethylene–Auxin Interactions Regulate Lateral Root Initiation and Emergence in Arabidopsis Thaliana." *The Plant Journal* 55(2):335–47. doi: 10.1111/j.1365-313X.2008.03528.x.
Khoury, Maleana G., R. Emily Martin, Maarten Houben, and Gloria K. Muday. 2024. "Ethylene Regulates Root Growth and Development." in *Plant Roots: The Hidden Half*. Boca Raton: CRC Press.
Kieber, Joseph J., Madge Rothenberg, Gregg Roman, Kenneth A. Feldmann, and Joseph R. Ecker. 1993. "CTR1, a Negative Regulator of the Ethylene Response Pathway in Arabidopsis, Encodes a Member of the Raf Family of Protein Kinases." *Cell* 72(3):427–41. doi: 10.1016/0092-8674(93)90119-B.

Kim, Heejung, Elizabeth E. Helmbrecht, M. Blaine Stalans, Christina Schmitt, Nesha Patel, Chi-Kuang Wen, Wuyi Wang, and Brad M. Binder. 2011. "Ethylene Receptor ETHYLENE RECEPTOR1 Domain Requirements for Ethylene Responses in Arabidopsis Seedlings." *Plant Physiology* 156(1):417–29. doi: 10.1104/pp.110.170621.

Kircher, Stefan, and Peter Schopfer. 2012. "Photosynthetic Sucrose Acts as Cotyledon-Derived Long-Distance Signal to Control Root Growth during Early Seedling Development in Arabidopsis." *Proceedings of the National Academy of Sciences* 109(28):11217–21. doi: 10.1073/pnas.1203746109.

Lakehal, Abdellah, Asma Dob, Zahra Rahneshan, Ondřej Novák, Sacha Escamez, Sanaria Alallaq, Miroslav Strnad, Hannele Tuominen, and Catherine Bellini. 2020. "ETHYLENE RESPONSE FACTOR 115 Integrates Jasmonate and Cytokinin Signaling Machineries to Repress Adventitious Rooting in Arabidopsis." *New Phytologist* 228(5):1611–26. doi: 10.1111/nph.16794.

Lee, S. H., and H. T. Cho. 2008. "Auxin and Root Hair Morphogenesis." Pp. 1–20 in *Plant Cell Monographs*. Berlin, Heidelberg: Springer Berlin Heidelberg.

Levesque, Mitchell P., Teva Vernoux, Wolfgang Busch, Hongchang Cui, Jean Y. Wang, Ikram Blilou, Hala Hassan, Keiji Nakajima, Noritaka Matsumoto, Jan U. Lohmann, Ben Scheres, and Philip N. Benfey. 2006. "Correction: Whole-Genome Analysis of the SHORT-ROOT Developmental Pathway in Arabidopsis." *PLOS Biology* 4(7):e249. doi: 10.1371/journal.pbio.0040249.

Lewis, Daniel R., Sangeeta Negi, Poornima Sukumar, and Gloria K. Muday. 2011. "Ethylene Inhibits Lateral Root Development, Increases IAA Transport and Expression of PIN3 and PIN7 Auxin Efflux Carriers." *Development* 138(16):3485–95. doi: 10.1242/dev.065102.

Love, Michael I., Wolfgang Huber, and Simon Anders. 2014. "Moderated Estimation of Fold Change and Dispersion for RNA-Seq Data with DESeq2." *Genome Biology* 15(12):550. doi: 10.1186/s13059-014-0550-8.

Ma, Qian, and Chun-Hai Dong. 2021. "Regulatory Functions and Molecular Mechanisms of Ethylene Receptors and Receptor-Associated Proteins in Higher Plants." *Plant Growth Regulation* 93(1):39–52. doi: 10.1007/s10725-020-00674-5.

Martin, Marcel. 2011. "Cutadapt Removes Adapter Sequences from High-Throughput Sequencing Reads." *EMBnet.Journal* 17:10–12.

Masucci, J. D., and J. W. Schiefelbein. 1996. "Hormones Act Downstream of TTG and GL2 to Promote Root Hair Outgrowth during Epidermis Development in the Arabidopsis Root." *The Plant Cell* 8(9):1505–17. doi: 10.1105/tpc.8.9.1505.

McDaniel, Brittany K., and Brad M. Binder. 2012. "Ethylene Receptor 1 (ETR1) Is Sufficient and Has the Predominant Role in Mediating Inhibition of Ethylene Responses by Silver in Arabidopsis Thaliana*." *Journal of Biological Chemistry* 287(31):26094–103. doi: 10.1074/jbc.M112.383034.

Mou, Wangshu, Yun-Ting Kao, Erwan Michard, Alexander A. Simon, Dongdong Li, Michael M. Wudick, Michael A. Lizzio, José A. Feijó, and Caren Chang. 2020. "Ethylene-Independent Signaling by the Ethylene Precursor ACC in Arabidopsis Ovular Pollen Tube Attraction." *Nature Communications* 11(1):4082. doi: 10.1038/s41467-020-17819-9.

Muday, Gloria K., Abidur Rahman, and Brad M. Binder. 2012. "Auxin and Ethylene: Collaborators or Competitors?" *Trends in Plant Science* 17(4):181–95. doi: 10.1016/j.tplants.2012.02.001.

Negi, Sangeeta, Maria G. Ivanchenko, and Gloria K. Muday. 2008. "Ethylene Regulates Lateral Root Formation and Auxin Transport in Arabidopsis Thaliana." *The Plant Journal* 55(2):175–87. doi: 10.1111/j.1365-313X.2008.03495.x.

O'Malley, Ronan C., Cesar C. Barragan, and Joseph R. Ecker. 2015. "A User's Guide to the Arabidopsis T-DNA Insertion Mutant Collections." *Methods in Molecular Biology (Clifton, N.J.)* 1284:323–42. doi: 10.1007/978-1-4939-2444-8_16.

O'Malley, Ronan C., Shao-Shan Carol Huang, Liang Song, Mathew G. Lewsey, Anna Bartlett, Joseph R. Nery, Mary Galli, Andrea Gallavotti, and Joseph R. Ecker. 2016. "Cistrome and Epicistrome Features Shape the Regulatory DNA Landscape." *Cell* 165(5):1280–92. doi:

10.1016/j.cell.2016.04.038.
Park, Min Young, Jung-youn Kang, and Soo Young Kim. 2011. "Overexpression of AtMYB52 Confers ABA Hypersensitivity and Drought Tolerance." *Molecules and Cells* 31(5):447–54. doi: 10.1007/s10059-011-0300-7.
Patro, Rob, Geet Duggal, Michael I. Love, Rafael A. Irizarry, and Carl Kingsford. 2017. "Salmon Provides Fast and Bias-Aware Quantification of Transcript Expression." *Nature Methods* 14(4):417–19. doi: 10.1038/nmeth.4197.
Qiao, Hong, Katherine N. Chang, Junshi Yazaki, and Joseph R. Ecker. 2009. "Interplay between Ethylene, ETP1/ETP2 F-Box Proteins, and Degradation of EIN2 Triggers Ethylene Responses in Arabidopsis." *Genes & Development* 23(4):512–21.
Qin, Hua, Lina He, and Rongfeng Huang. 2019. "The Coordination of Ethylene and Other Hormones in Primary Root Development." *Frontiers in Plant Science* 10.
Rahman, Abidur, Seiji Tsurumi, Taisaku Amakawa, Kouichi Soga, Takayuki Hoson, Nobuharu Goto, and Seiichiro Kamisaka. 2000. "Involvement of Ethylene and Gibberellin Signalings in Chromosaponin I-Induced Cell Division and Cell Elongation in the Roots of Arabidopsis Seedlings." *Plant and Cell Physiology* 41(1):1–9. doi: 10.1093/pcp/41.1.1.
Ritchie, Matthew E., Belinda Phipson, Di Wu, Yifang Hu, Charity W. Law, Wei Shi, and Gordon K. Smyth. 2015. "Limma Powers Differential Expression Analyses for RNA-Sequencing and Microarray Studies." *Nucleic Acids Research* 43(7):e47–e47. doi: 10.1093/nar/gkv007.
Růžička, Kamil, Karin Ljung, Steffen Vanneste, Radka Podhorská, Tom Beeckman, Jiří Friml, and Eva Benková. 2007. "Ethylene Regulates Root Growth through Effects on Auxin Biosynthesis and Transport-Dependent Auxin Distribution." *The Plant Cell* 19(7):2197–2212. doi: 10.1105/tpc.107.052126.
Sakai, Hajime, Jian Hua, Qianhong G. Chen, Caren Chang, Leonard J. Medrano, Anthony B. Bleecker, and Elliot M. Meyerowitz. 1998. "ETR2 Is an ETR1-like Gene Involved in Ethylene Signaling in Arabidopsis." *Proceedings of the National Academy of Sciences* 95(10):5812–17. doi: 10.1073/pnas.95.10.5812.
Schaller, G. Eric, and Anthony B. Bleecker. 1995. "Ethylene-Binding Sites Generated in Yeast Expressing the Arabidopsis ETR1 Gene." *Science* 270(5243):1809–11.
Schaller, G. Eric, and Joseph G. Kieber. 2002. "Ethylene." *The Arabidopsis Book* 2002(1). doi: 10.1199/tab.0071.
Shakeel, Samina N., Xiaomin Wang, Brad M. Binder, and G. Eric Schaller. 2013. "Mechanisms of Signal Transduction by Ethylene: Overlapping and Non-Overlapping Signalling Roles in a Receptor Family." *AoB PLANTS* 5:plt010. doi: 10.1093/aobpla/plt010.
Singh, Sharmila, Sandeep Yadav, Alka Singh, Mahima Mahima, Archita Singh, Vibhav Gautam, and Ananda K. Sarkar. 2020. "Auxin Signaling Modulates LATERAL ROOT PRIMORDIUM1 (LRP1) Expression during Lateral Root Development in Arabidopsis." *The Plant Journal* 101(1):87–100. doi: 10.1111/tpj.14520.
Soneson, Charlotte, Katarina L. Matthes, Malgorzata Nowicka, Charity W. Law, and Mark D. Robinson. 2016. "Isoform Prefiltering Improves Performance of Count-Based Methods for Analysis of Differential Transcript Usage." *Genome Biology* 17(1):12. doi: 10.1186/s13059-015-0862-3.
Stepanova, Anna N., Jeonga Yun, Alla V. Likhacheva, and Jose M. Alonso. 2007. "Multilevel Interactions between Ethylene and Auxin in Arabidopsis Roots." *The Plant Cell* 19(7):2169–85. doi: 10.1105/tpc.107.052068.
Stephens, Matthew, Peter Carbonetto, David Gerard, Mengyin Lu, Lei Sun, Jason Willwerscheid, and Nan Xiao. 2020. "Methods for Adaptive Shrinkage, Using Empirical Bayes [R Package Ashr Version 2.2-47]."
Tian, Tian, Yue Liu, Hengyu Yan, Qi You, Xin Yi, Zhou Du, Wenying Xu, and Zhen Su. 2017. "agriGO v2.0: A GO Analysis Toolkit for the Agricultural Community, 2017 Update." *Nucleic Acids Research* 45(W1):W122–29. doi: 10.1093/nar/gkx382.
Van de Poel, Bram, Dajo Smet, and Dominique Van Der Straeten. 2015. "Ethylene and Hormonal Cross

Talk in Vegetative Growth and Development." *Plant Physiology* 169(1):61–72. doi: 10.1104/pp.15.00724.

Vanderstraeten, Lisa, Thomas Depaepe, Sophie Bertrand, and Dominique Van Der Straeten. 2019. "The Ethylene Precursor ACC Affects Early Vegetative Development Independently of Ethylene Signaling." *Frontiers in Plant Science* 10.

Wang, Kevin L. C., Hai Li, and Joseph R. Ecker. 2002. "Ethylene Biosynthesis and Signaling Networks." *The Plant Cell* 14(suppl_1):S131–51. doi: 10.1105/tpc.001768.

Wickham, Hadley. 2016. *Ggplot2: Elegant Graphics for Data Analysis*. 2nd ed. Springer Cham.

Wingett, SW, and S. Andrews. 2018. "FastQ Screen: A Tool for Multi-Genome Mapping and Quality Control [Version 2; Peer Review: 4 Approved]." *F1000Research* 7(1338). doi: 10.12688/f1000research.15931.2.

Yin, Jiao, Xiaoqian Zhang, Gensong Zhang, Yuanyuan Wen, Gang Liang, and Xiaolan Chen. 2019. "Aminocyclopropane-1-Carboxylic Acid Is a Key Regulator of Guard Mother Cell Terminal Division in Arabidopsis Thaliana." *Journal of Experimental Botany* 70(3):897–908. doi: 10.1093/jxb/ery413.

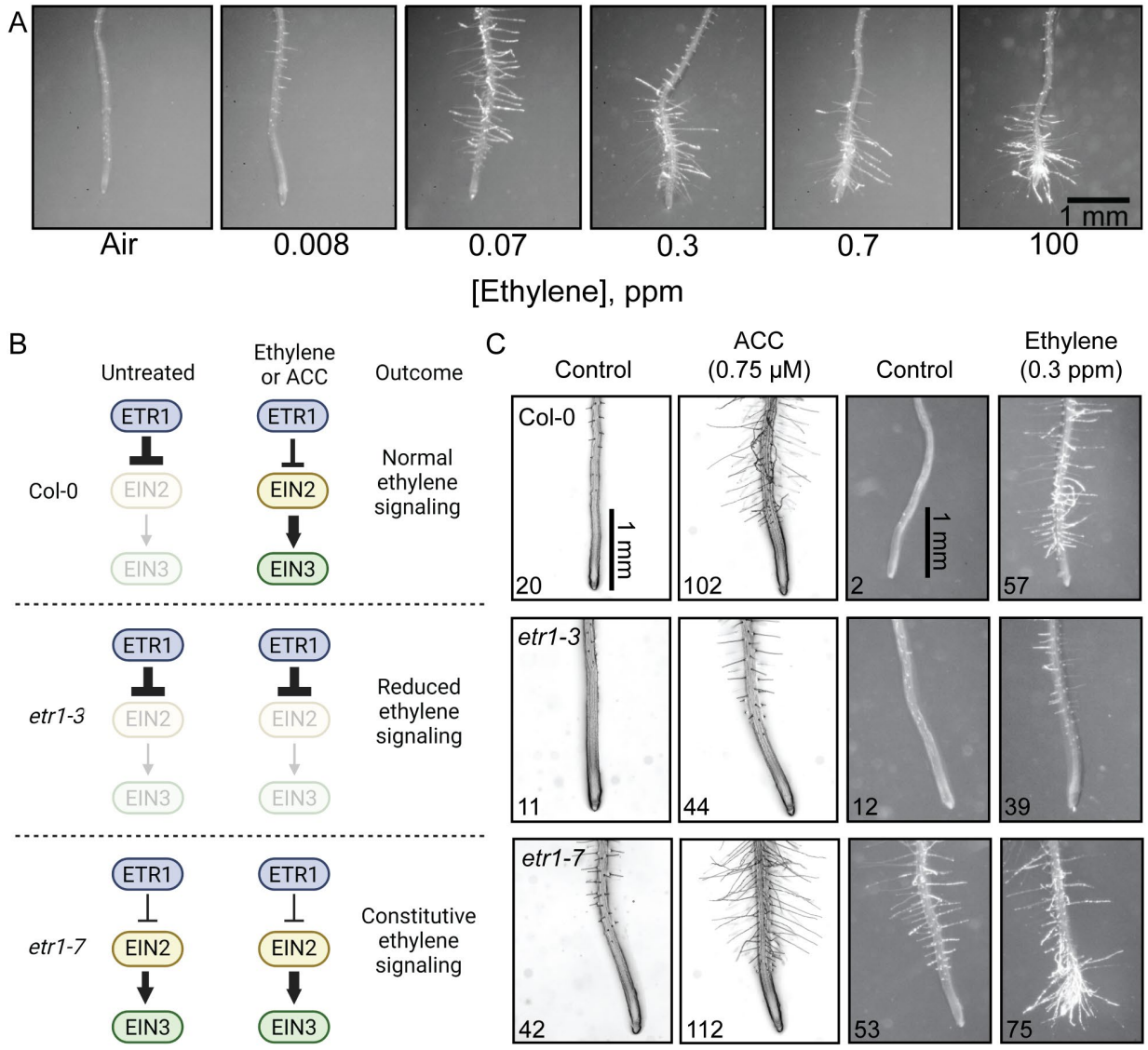

Figure 1. Ethylene and ACC both induce root hair proliferation. (A) Representative images of five-day-old seedlings treated with the indicated dose of ethylene for 24 hours. (B) Representative images of five-day-old Col-0, *etr1-3*, and *etr1-7* seedlings treated with 0.3 ppm ethylene or 0.75 μM ACC for 24 hours, revealing similar developmental responses by these two doses of ethylene and ACC within the different genotypes. Numbers indicate the total number of root hairs quantified in each image.

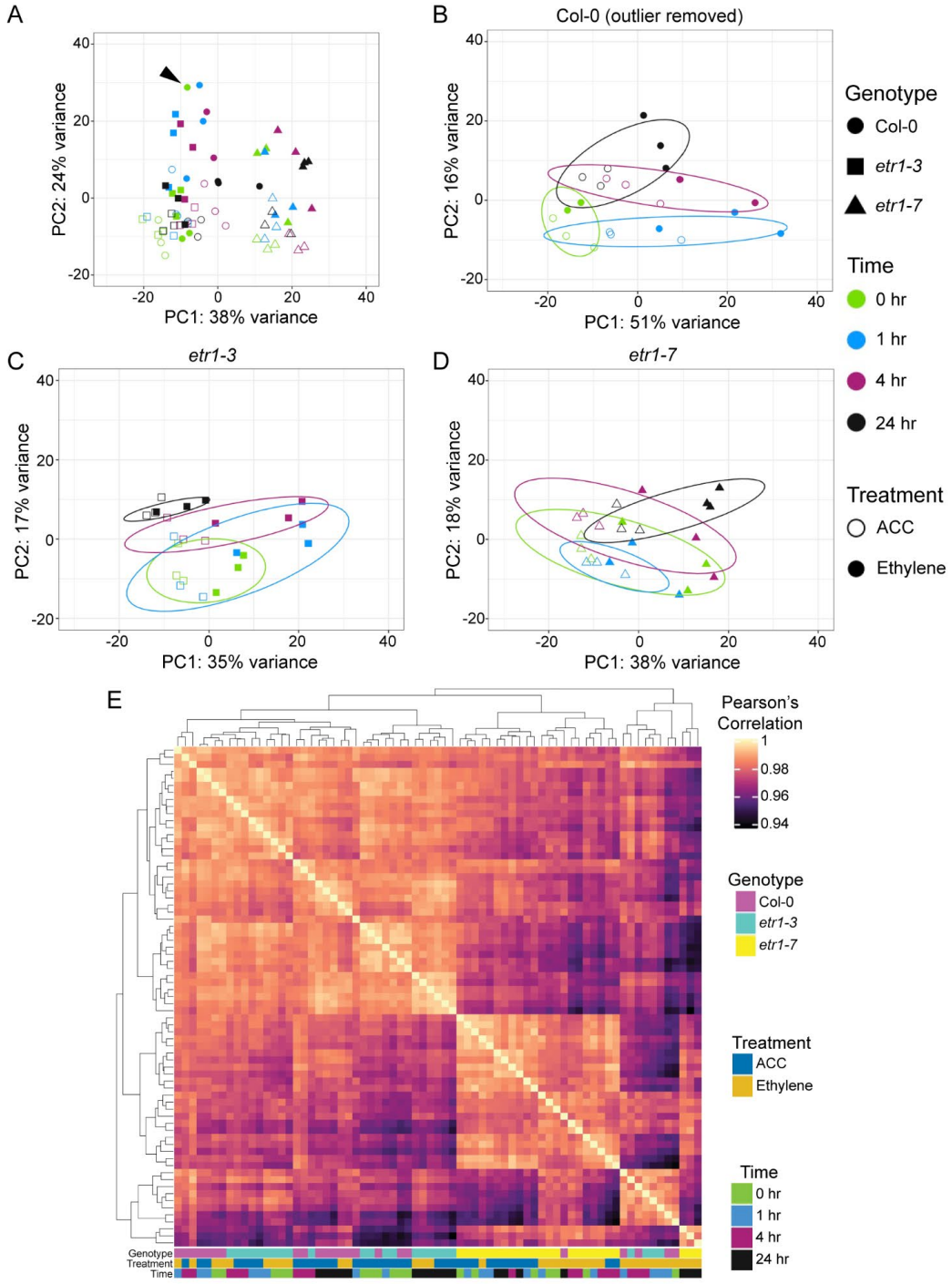

Figure 2. Large-scale transcript abundance patterns in data show *etr1-7* samples are distinctly different from Col-0 and *etr1-3*. (A) PCA plot of all sequenced samples. Arrow denotes Col-0 time 0 outlier. PCA plots of (B) Col-0 (with the outlier sample removed), (C) *etr1-3*, and (D) *etr1-7* samples. Circles surround the 80% confidence intervals for each time point. (E) Pearson Correlation plot for all samples.

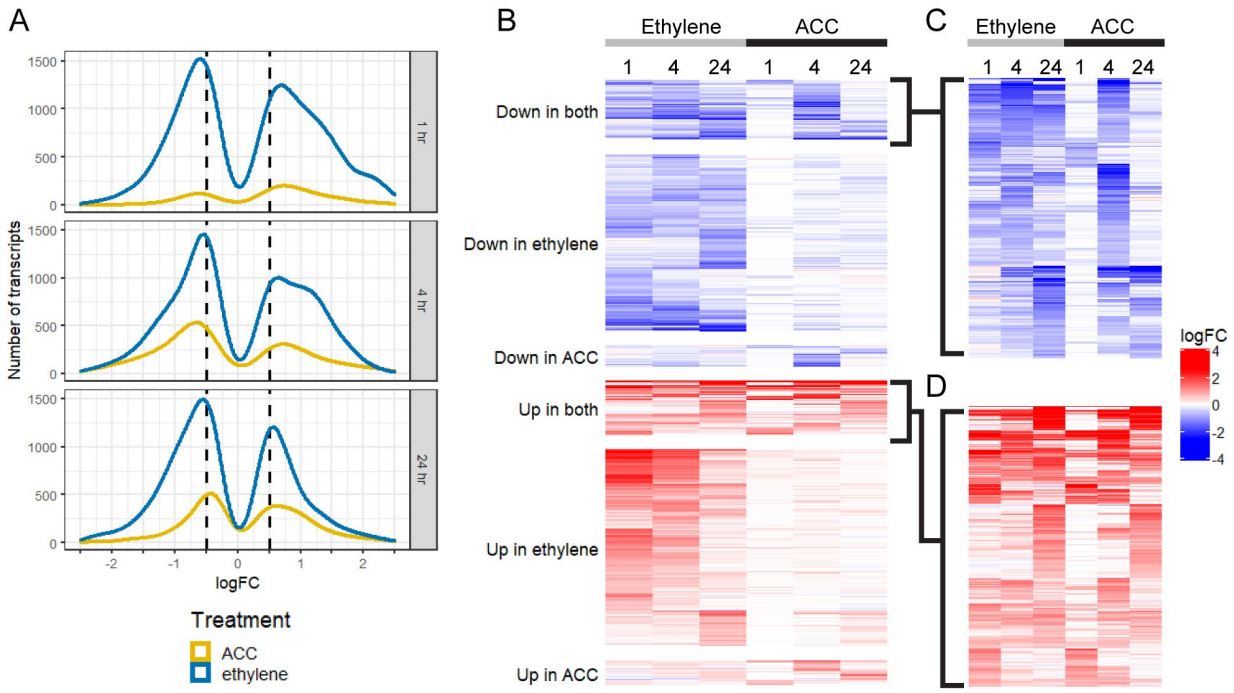

Figure 3. The transcriptional responses to ethylene and ACC treatment revealed more down-regulated genes at 4 and 24 hours and more DE genes by ethylene than ACC. (A) Density plot reporting the number of transcripts across a range of logFC values for each treatment and time point in Col-0 samples. The logFC is relative to Col-0 control (time 0). For each treatment and time point, only transcripts with an adjusted p-value < 0.01 are shown; no logFC cutoff was used. (B) This heatmap shows the ratios of all transcripts relative to untreated Col-0 samples, that are DE in at least one Col-0 sample treated with ethylene or ACC with |logFC| > 0.5 and adjusted p-value < 0.01. logFC for all columns is relative to Col-0 control (time 0) samples. (C & D) Transcripts which are DE in at least one time point for both ethylene and ACC, with a (C) negative or (D) positive logFC.

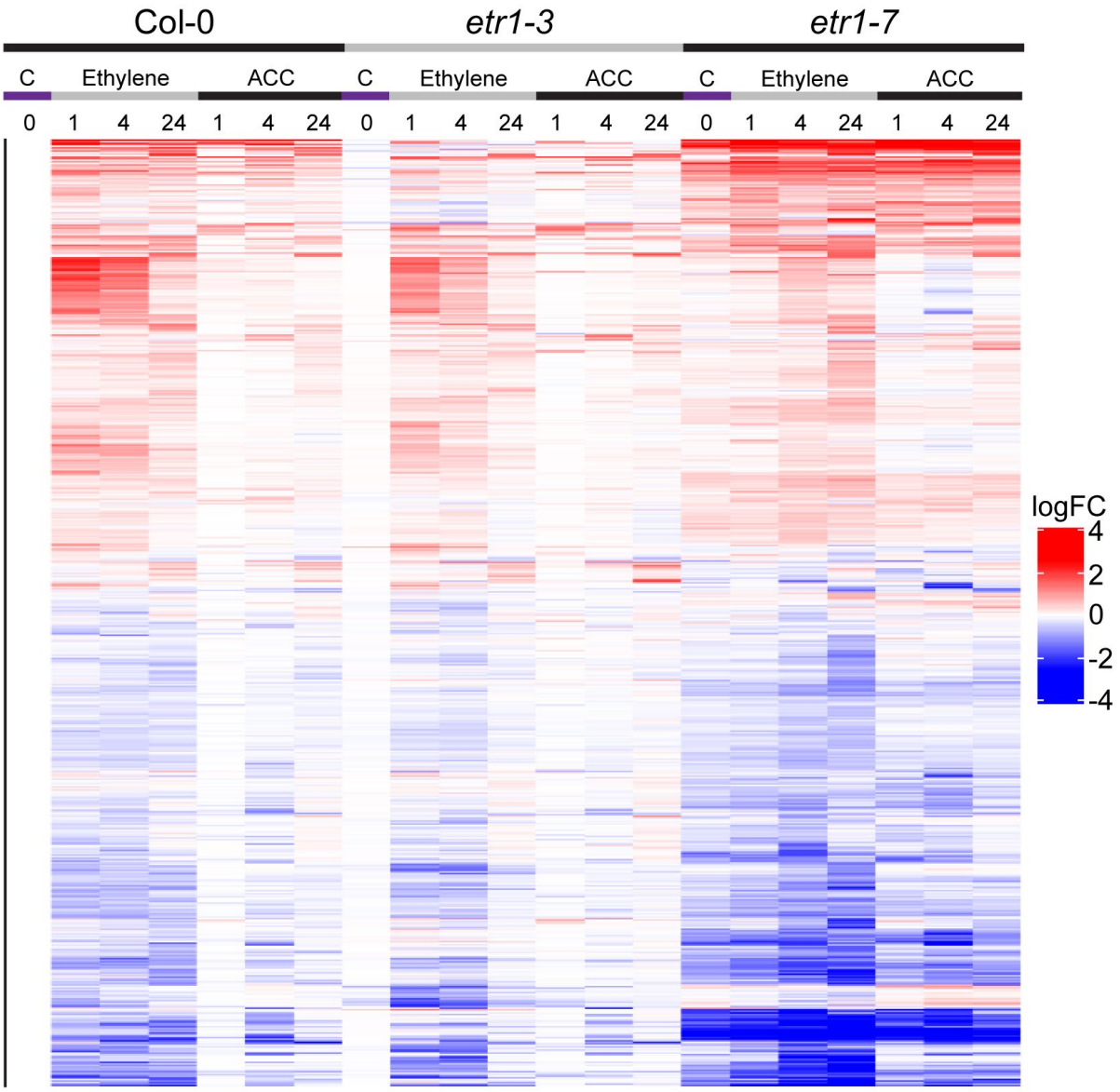

Figure 4. Heatmap of all transcripts that were DE in at least one time point, treatment, or genotype revealed a variety of patterns. This comparison of the transcriptional responses across treatments, time points and genotypes revealed suppressed ethylene signaling in *etr1-3* and enhanced ethylene signaling in *etr1-7*, relative to Col-0 untreated. The heat map includes all 8,323 transcripts that are DE in at least one of the represented groups in comparison with Col-0 control with |logFC| > 0.5 and adjusted p-value < 0.01. logFC for all columns is relative to Col-0 control (time 0) samples.

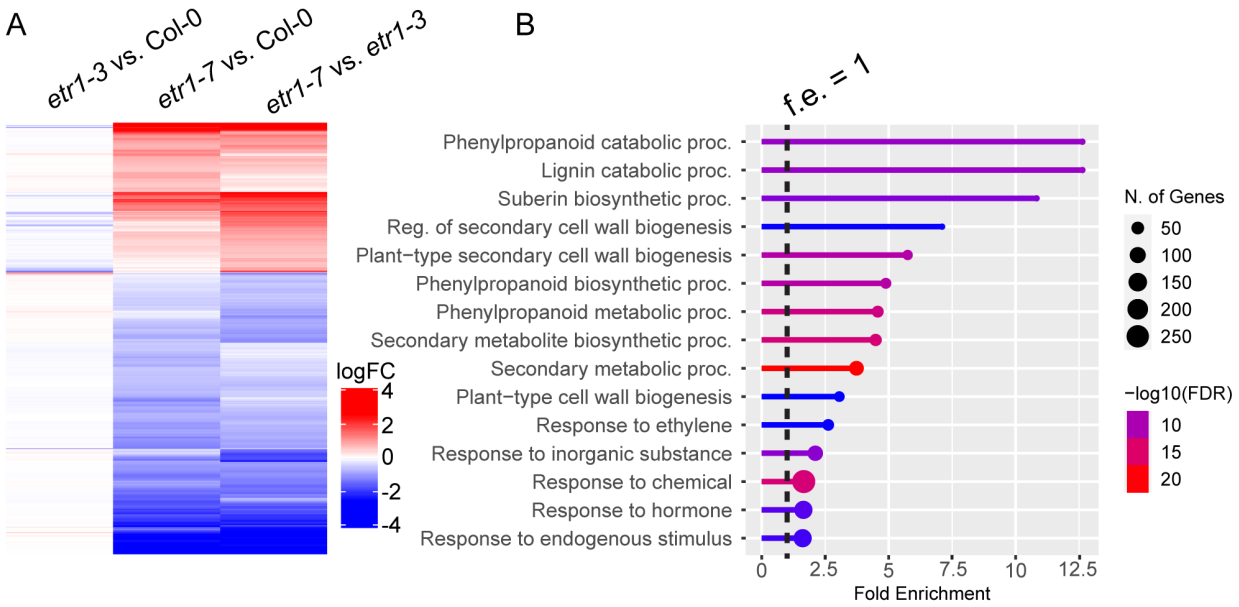

Figure 5. Baseline transcript abundance differences between Col-0 and the *etr1* mutants were consistent with constitutive ethylene signaling in *etr1-7*. (A) All transcripts which are DE in at least one comparison with |logFC| > 0.5 and adjusted p-value < 0.01. logFC is relative to the second genotype in each comparison. (B) Enriched biological processes among the 1,458 DE genes in the overlap between the *etr1-7* vs. Col-0 comparisons and the *etr1-7* vs. *etr1-3* comparisons as determined by ShinyGO 0.80 (Ge, Jung, and Yao 2020).

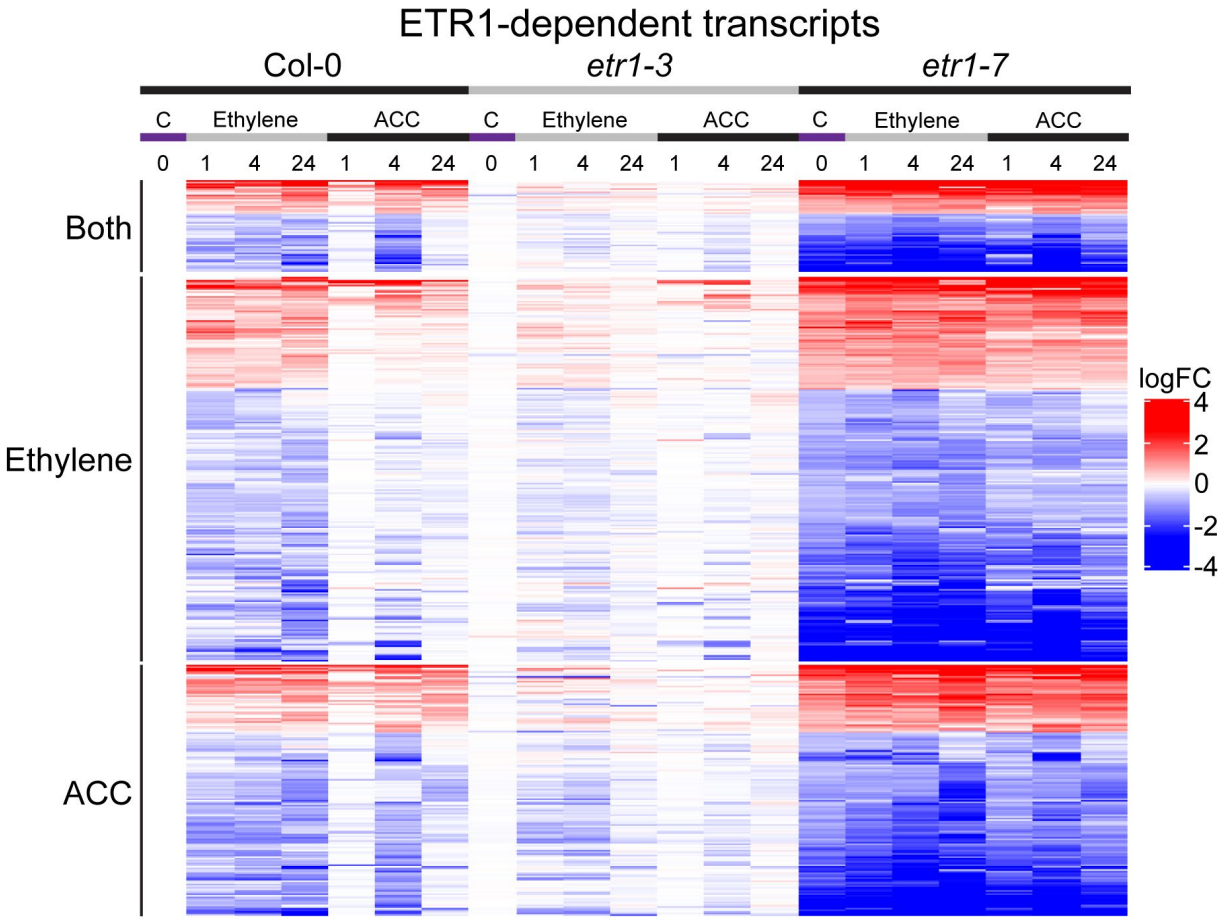

Figure 6. ETR1-dependent transcript heatmap revealed genotype and treatment dependent changes in transcript abundance. This comparison of transcript abundance across treatments and genotypes revealed a set of transcripts that responded to ethylene and/or ACC treatment in Col-0 but not in the mutants. Transcripts which follow a pattern of response that suggests they are ETR1-dependent were selected. These transcripts respond to ACC and/or ethylene treatment in Col-0, do not respond in *etr1-3*, and are constitutively up or down in *etr1-7*, based on |logFC| > 0.5 and adjusted p-value < 0.01. The logFC reported here was determined relative to Col-0 control (time 0). Genes are split into three groups, based on whether they met our ETR1-dependent criteria in ethylene only, in ACC only, or in both treatments.

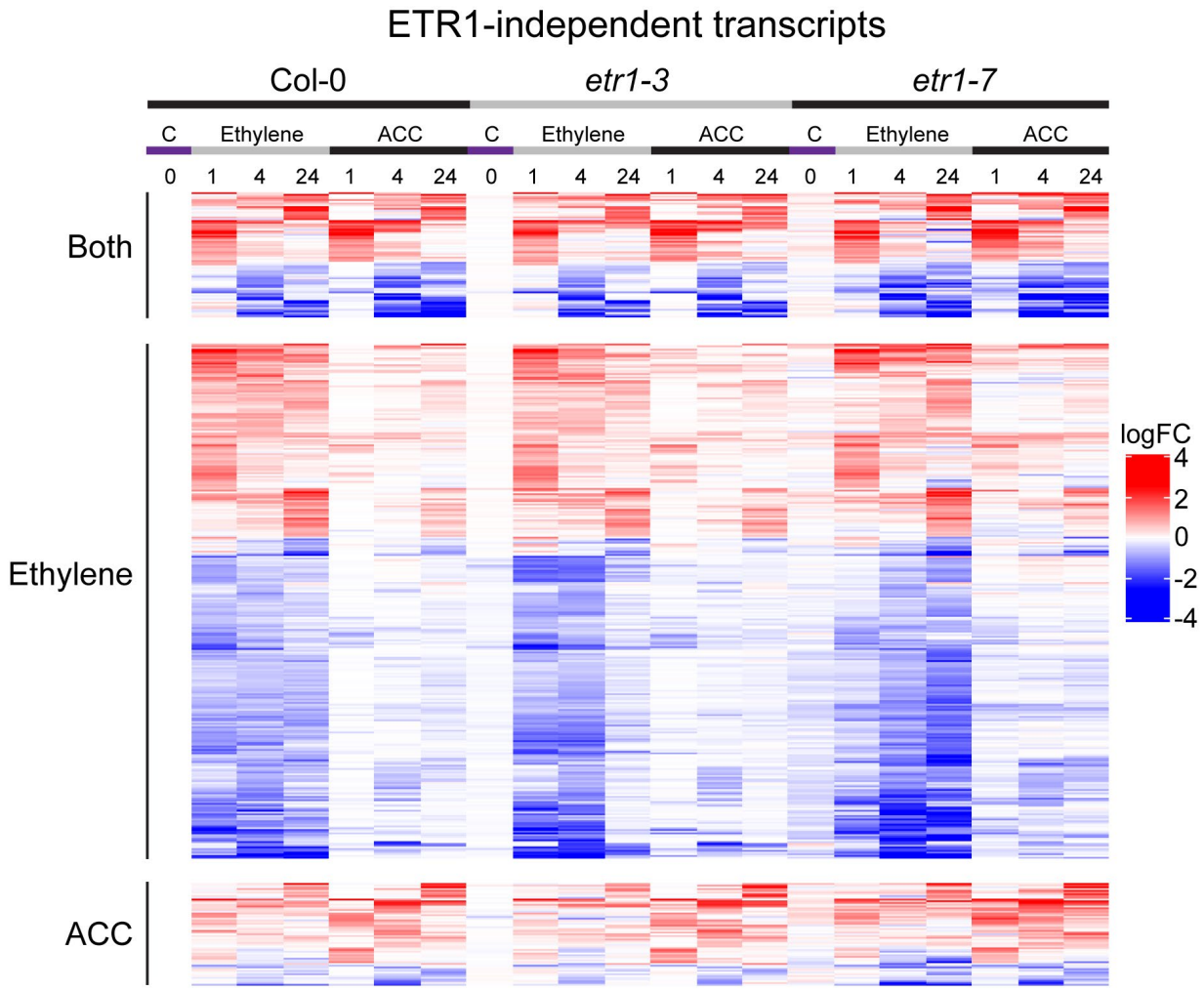

Figure 7. ETR1-independent transcript heatmap revealed genotype and treatment independent changes in transcript abundance. This comparison of transcript abundance across treatments and genotypes revealed a set of genes that responded to ethylene and/or ACC treatment in all genotypes. Genes which respond to ethylene or ACC in all three genotypes were considered receptor-independent (since transcript abundance should have been constant in *etr1-3* and *etr1-7)*. Significant differences were defined as having |logFC| > 0.5 and adjusted p-value < 0.01. Transcripts are divided based on which treatment qualifies as ETR1-independent. logFC is reported relative to Col-0 control (time 0). Genes are split into three groups, based on whether they met our ETR1-independent criteria in ethylene only, in ACC only, or in both treatments.

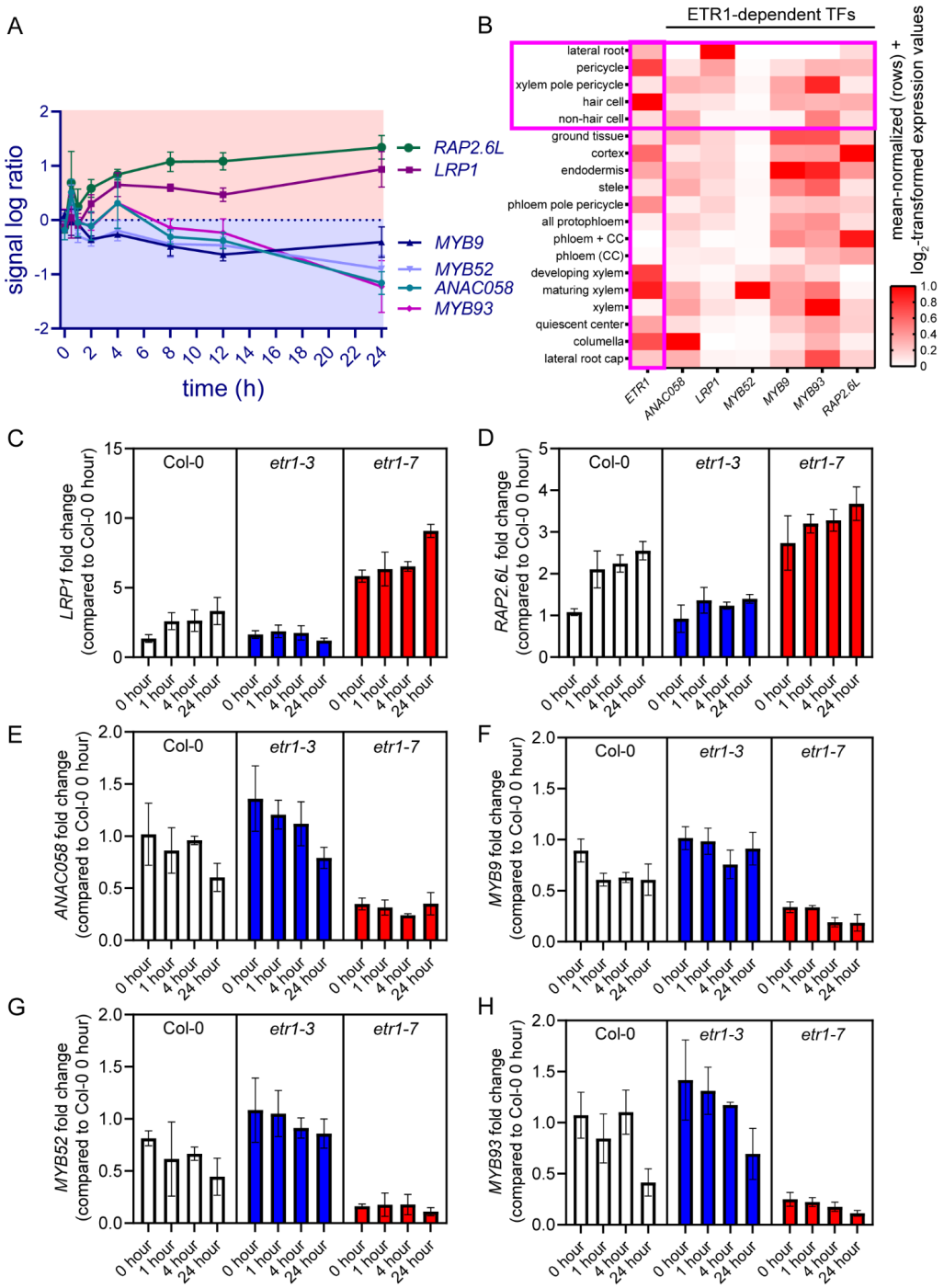

Figure 8. Transcript abundance patterns for the six ETR1-dependent TFs. (A) The signal log ratios over time after ACC treatment were reported (Harkey et al. 2018). (B) Cell-type-specific data is from (Brady et al. 2007). Expression values were mean-normalized (rows) and $\log_2$-transformed. CC, companion cell. (C-H) Fold change of normalized transcript abundance of these six genes in the *etr1-3* and *etr1-7* mutants relative to Col-0 in the absence of treatment with hormone. Error bars represent standard deviation across 2-3 three biological replicates.

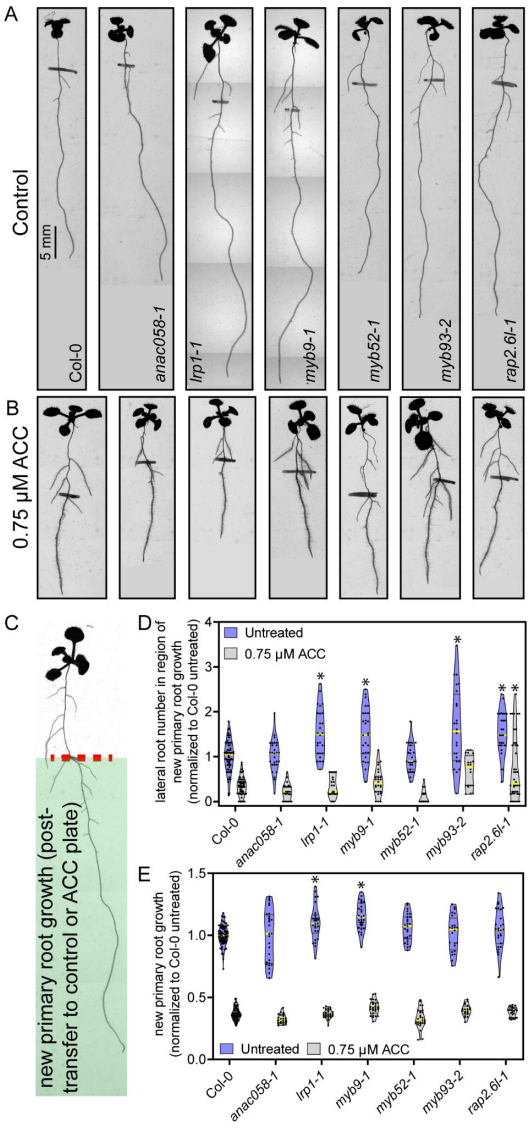

Figure 9. Mutant screens revealed ETR1-dependent TFs that functioned in lateral root formation or primary root growth. (A and B) Representative images of 10-day-old seedlings five days after transfer to plates without ACC (A) or with 0.75 µM ACC (B). The black horizontal marks indicate where the primary root tips were right after transfer to treatment or control plates. (C) Diagram of regions of root quantification. (D) Violin plot of the lateral root number in the region of new root growth in the absence and presence of 0.75 µM ACC normalized to Col-0 untreated. (E) Violin plot showing the length of new primary root growth in millimeters in the absence and presence of 0.75 µM ACC normalized to Col-0 untreated. Asterisks indicate significant difference from Col-0 under the same conditions (without or with ACC) ($P < 0.05$). ACC effects within genotypes were significant for all genotypes ($P < 0.05$). Three biological replicates were performed. The median is shown in a thicker yellow line. The quartiles are shown in thinner gray lines.

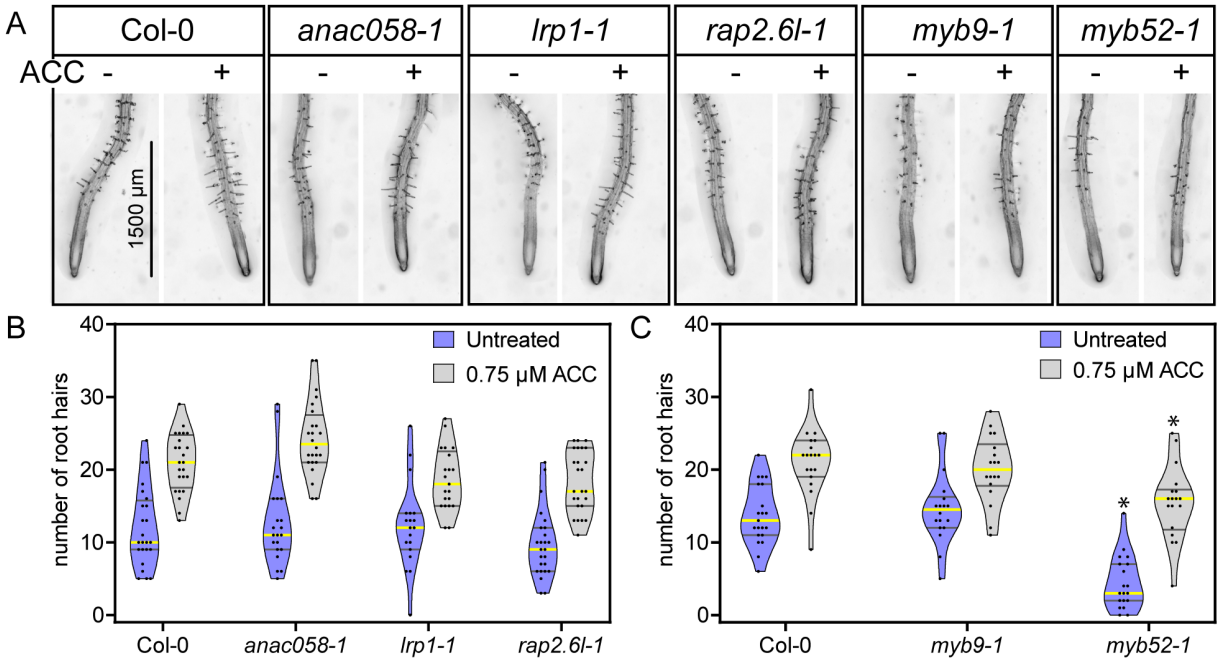

Figure 10. Mutant screens revealed ETR1-dependent TFs that functioned in root hair initiation. (A) Representative images of five-day-old Col-0 and mutant seedlings treated with and without ACC for four hours with a size bar of 1,500 µM. (B) Violin plot of the number of root hairs in the region 0-1500 µm from the root tip in the absence and presence of 0.75 µM ACC for time-matched Col-0, *anac058-1*, *lrp1-1* and *rap2.6l-1*. (C) Violin plot of the number of root hairs in the region 0-1500 µm from the root tip in the absence and presence of 0.75 µM ACC for time-matched Col-0, *myb9-1*, and *myb52-1*. Asterisks indicate significant difference from Col-0 under similar conditions, either untreated or with ACC ($P < 0.05$). ACC effects within genotypes were significant for all genotypes ($P < 0.05$). Three biological replicates were performed. The median is shown in a thicker yellow line. The quartiles are shown in thinner gray lines. Root hair data for *myb93-2* were reported in Supplemental Figure 8.

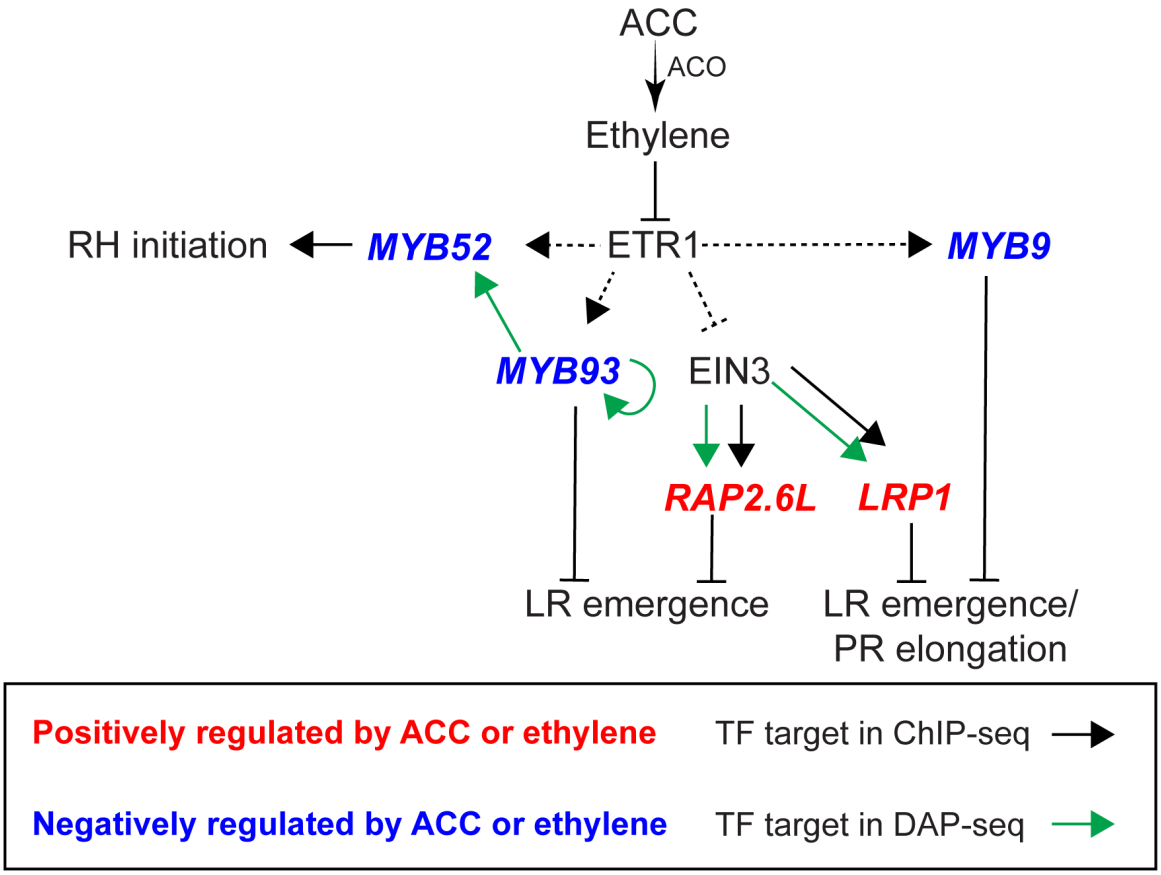

Figure 11. Model for ETR1-dependent control of root hair and lateral root formation with overlaid publicly available ChIP-seq and DAP-seq data. The dotted arrows and inhibition symbols indicate an indirect relationship between the ETR1 receptor and its downstream targets. ACC, 1 aminocyclopropane-1-carboxylic acid; ACO, ACC oxidase; ETR1, ETHYLENE RESPONSE 1 (ethylene receptor); *EIN3*, *ETHYLENE INSENSITIVE 3; LRP1, LATERAL ROOT PRIMORDIUM 1*; *MYB9*, *MYB DOMAIN PROTEIN 9*; *MYB52*, *MYB DOMAIN PROTEIN 52*; *MYB93*, *MYB DOMAIN PROTEIN 93*; LRP1, LATERAL ROOT PRIMORDIUM 1; *RAP2.6L*, *RELATED TO AP2 6L*; LR, lateral root; PR, primary root. ChIP-Seq data was from (Chang et al. 2013) and DAP-Seq data was from (O'Malley et al. 2016). *NAC058* was not shown as it did not have a root phenotype, but its protein binds to the promoter of *MYB52* according to the DAP-Seq data.